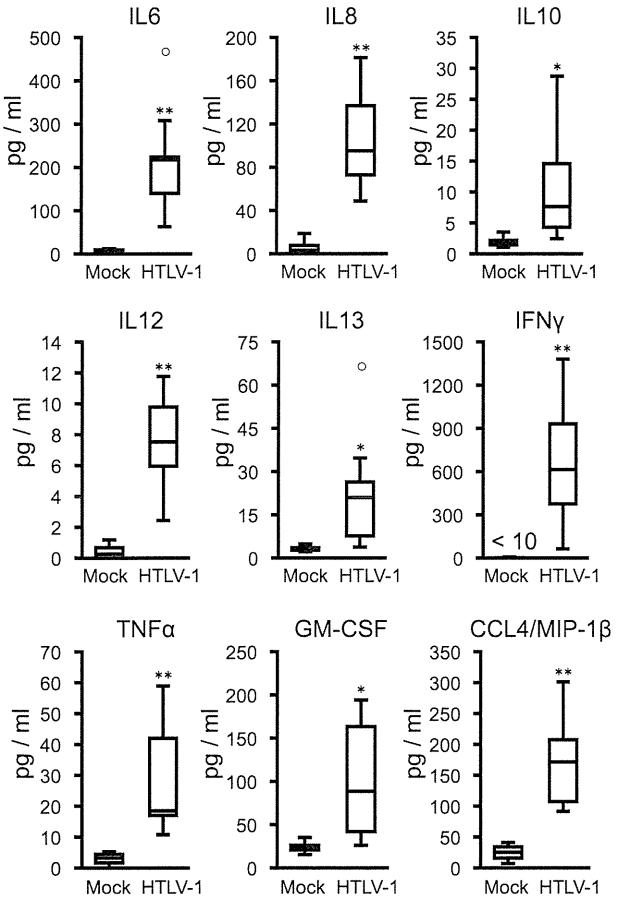

Figure 4. Induction of inflammatory cytokines in infected IBMI-huNOG mice. Human cytokine concentrations in plasma. Plasma was collected following sacrifice of mock-infected (n = 4) and HTLV-1–infected mice (n = 8). Seventeen cytokines were quantified using a cytokine bead array system. The concentrations of human IL-6, IL-8, IL-10, IL-12, IL-13, IFNγ, TNF-α, GM-CSF, and CCL4/MIP-1β are shown, all of which were significantly increased in the plasma of HTLV-1–infected mice. Increased expressions of the other 6 cytokines (IL-2, IL-4, IL-7, IL-17, G-CSF, and MCP-1) were also observed in infected mice but not statistically significant. On the other hand, little decrease in the concentrations of IL-1 and IL-5 was seen. Asterisks in each panel represent significant differences vs mock-infected mice (*$P < .05$, **$P < .01$ by Mann-Whitney U test).

human stem cells directly into the bone marrow cavity of NOD/Shi-SCID/IL-2Rγc null (NOG) mice using an IBMI method.

The efficacy of humanization achieved in this model is markedly superior to other procedures, such as intrahepatic or intravenous injection of human hematopoietic stem cells.[21,22,29] While T-lineage–cell populations become dominant over B-cell populations in the lymphoid organs of other humanized mouse systems within a few months after transplantation, in IBMI-huNOG mice the B-to-T-cell ratio remained constant for >8 months posttransplantation (Figure 1E). One possible explanation for this difference is that direct injection of hematopoietic stem cell preparations into the bone marrow of recipient mice improves the colonization efficiency of long-term stem cells.[27,46] Moreover, we used $CD133^+$ cells to generate IBMI-huNOG mice. CD133, the early hematopoietic progenitor cell marker, is thought to be ancestral to CD34 in human hematopoiesis.[47] Previous studies have revealed that $CD133^+$ cells were capable of differentiating not only into hematopoietic cells but also into endothelial, stromal, neuronal, and other type of cells.[47-49] It is possible that human mesenchymal stromal cells derived from $CD133^+$ cells support the development and maintenance of human B cells in the bone marrow microenvironment.

Having established a new humanized mouse model, we then infected IBMI-huNOG mice with HTLV-1 through inoculation with sublethally irradiated HTLV-1–producing cells.[28] HTLV-1–infected IBMI-huNOG mice recapitulated a large number of pathological features characteristic of ATL patients, including hyperproliferation of $CD3^+$ T cells, clonal proliferation of $CD25^+$ CD4 T cells, the appearance of flower cells in the periphery, hepatosplenomegaly, inflammatory hypercytokinemia, and down-regulation of CD3 on T cells.

Overgrowth of infected T cells was correlated with the expression of CD25 on CD4 T cells, consistent with recent reports.[17] However, the substantial proportion of $CD25^-$ CD4 T cells were also infected and identical T-cell clones, as determined by provirus integration site, were detected as the most abundant clones in both $CD25^-$ and $CD25^+$ CD4 T-cell populations, suggesting that CD25 expression likely occurs after infection in the course of clonal expansion. In addition, the expressions of *tax* and CD25 were inversely correlated. Further research will be necessary to identify molecular events associated with the suppression of *tax* expression in HTLV-1–infected $CD25^+$ CD4 T cells in relation to the development of ATL.

Banerjee et al[16] described the development of T-cell lymphoma following bone marrow transplantation of HTLV-1–infected $CD34^+/CD38^-$ hematopoietic stem cells into a NOD/SCID mouse. The lymphoma cells in these mice were capable of infiltrating into multiple organs but represented only $CD25^-$ or $CD25^{low}$ phenotypes. In contrast, HTLV-1–infected IBMI-huNOG mice developed leukemia in $CD25^+$ CD4 T cells, similar to that observed in ATL patients. The mechanism underlying this difference is unknown but may be due to differences in the developmental stage of T cells at the time of infection. Indeed, HTLV-1 infection in a different humanized mouse model, generated by intrahepatic transplantation of human $CD34^+$ stem cells into $Rag2^{-/-}\gamma c^{-/-}$ mice, induced formation of thymomas/lymphomas in mature CD4 T cells.[17] In this case, HTLV-1 infection was carried out 4 and 8 weeks after transplantation of $CD34^+$ hematopoietic stem cells, giving the human immune system time to develop. Thus the infection of $CD34^+$ stem cells per se does not appear to be sufficient for the induction of mature $CD25^+$ T cell malignancies and may require more developed lymphoid cells or a more appropriate microenvironment capable of supporting cell development.

Furthermore, HTLV-1–infected IBMI-huNOG mice almost exclusively developed leukemia, whereas HTLV-1 infection in the other humanized mouse models described above preferentially induced formation of lymphoma or thymoma. The reason for this difference is not clear but may stem from differences in the timing of T-cell infection. IBMI-huNOG mice were infected after the human hematopoietic system had been fully established, while in the other systems the infection was carried out before or shortly after stem cell transplantation.

In addition to leukemic growth of $CD25^+$ T cells, we also observed formation of flower cells in the peripheral blood of infected mice at later time points postinfection (>16 wpi). Although transformed T cells derived from Tax-transgenic mice were found to exhibit similar morphology,[15] none of the animal models described so far had recapitulated this pathology. Clonal analysis performed as part of this study demonstrated that the expansion of $CD25^+$ T-cell clones preceded the appearance of flower cells in periphery, suggesting a sequence of events that occurs during development of the malignancy. Thus, chronological

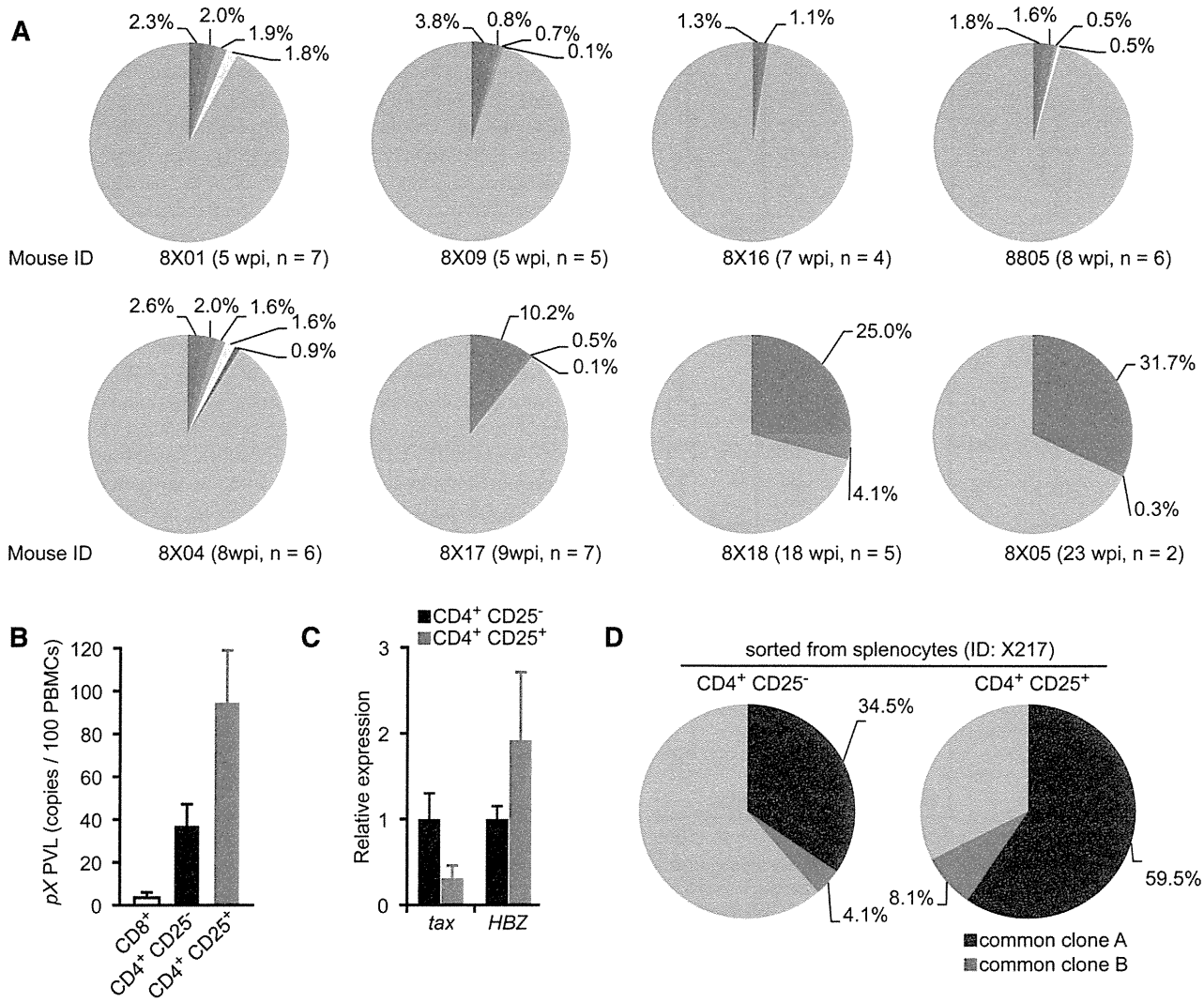

Figure 5. Progression of clonality in splenocytes of infected IBMI-huNOG. (A) Occupancy of HTLV-1–infected clones in the spleen. Abundant integration sites of HTLV-1 provirus were amplified by IL-PCR and subcloned into plasmids. The number of integration sites in each splenic DNA sample was determined by quantitative PCR using the clone-specific nucleotide sequence for each integration site. Results from 8 individual HTLV-1–infected mice are shown as pie charts. Size of the slice is proportional to the relative abundance of T-cell clones successfully amplified by IL-PCR, while data of minor clones with less than 0.1% occupancy were omitted. Gray regions represent clones with undefined integration sites. n, number of integration sites determined by nucleotide sequence of cloned PCR fragments in each mouse. (B) PVLs of specifiedT-cell populations. Splenocytes from HTLV-1–infected mice (n = 5) were sorted into $CD25^-$ or $CD25^+$ CD4 T cells and $CD8^+$ T cells. Genomic DNA isolated from each T-cell population was analyzed for PVL by real-time PCR using primers for the *pX* region of HTLV-1. (C) Comparative analysis of viral transcripts in $CD25^-$ and $CD25^+$ CD4 T-cell populations. Splenocytes from HTLV-1–infected mice (n = 5) are identical to those in mentioned above. The expression levels of *tax* (left) and *HBZ* (right) were analyzed by quantitative RT-PCR and were normalized to that of *HPRT1*. Results are presented as the fold change compared with the value in $CD25^-$ CD4 T cells. (D) Detection of common T-cell clones in the $CD25^-$ and $CD25^+$ CD4 T-cell populations. Clonal occupancy in both $CD25^-$ and $CD25^+$ populations are presented as pie charts. Two abundant common clones were analyzed for occupancy. Identified integration sites are listed in supplemental Table 5. The purity of each sorted population was >95% (supplemental Figure 3).

analysis of genetic and/or biochemical events in infected T cells from this mouse model should provide substantial information regarding the development of ATL.

We detected HLA-restricted CTLs against Tax protein of HTLV-1, as demonstrated in the peripheral blood of HTLV-1–infected carriers,[43] confirming the presence of an acquired immune response. Furthermore, the frequency of CTLs in CD8 T-cell populations were inversely correlated with the number of infected T cells in the spleen of humanized mice, similar to observations in HTLV-1–infected individuals.[43] The presence of functional T cells was also supported by the production of IgG antibodies specific to HTLV-1. Although humanized mice established by the transplantation of $CD34^+$ hematopoietic stem cells have been reported to produce antibodies against specific pathogens such as EBV,[22] HIV-1,[21] and DENV,[50] class switching from IgM to IgG was observed in only a few cases, likely due to immature T-cell development. In the IBMI-huNOG system, however, IgG production against HTLV-1 structural protein was observed after biphasic induction of antibodies after 8 weeks, indicating a functional interaction between CD4 T cells and B cells specific for viral antigens. Taken together, these data demonstrate induction of an adaptive immune response against HTLV-1 in HTLV-1–infected IBMI-huNOG mice, which may play an important role as selective pressure in the expansion of malignant T-cell clones.

In conclusion, our study demonstrates that the HTLV-1–infected IBMI-huNOG mouse represents a novel model that will facilitate elucidation of the molecular mechanism of in vivo development of ATL. Moreover, our model can also be used to develop and evaluate

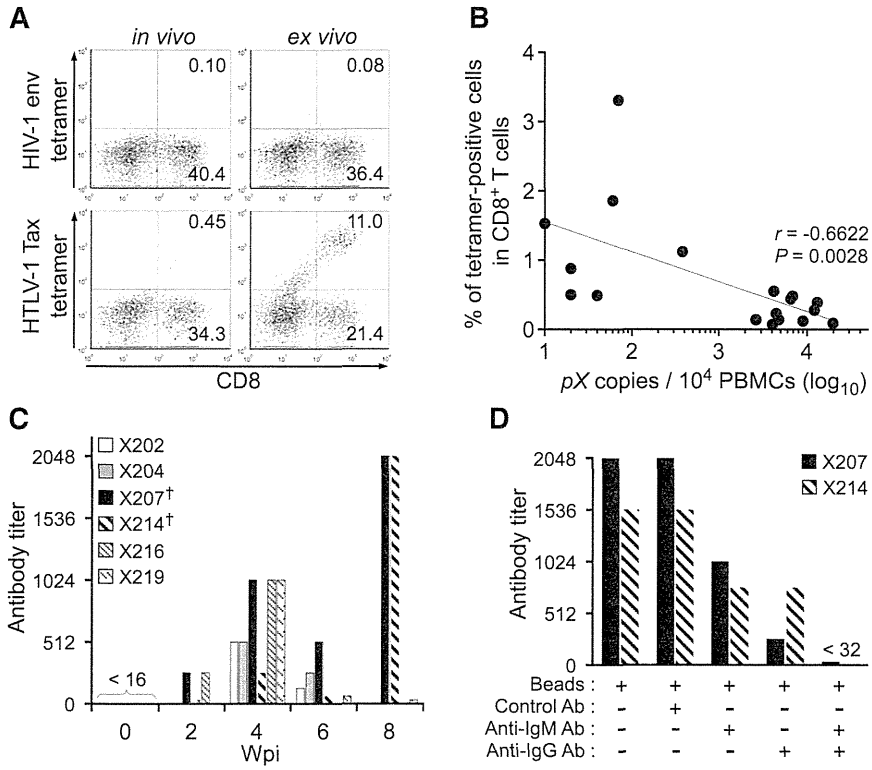

Figure 6. Induction of cellular and humoral immune responses against HTLV-1 in infected IBMI-huNOG mice. (A) Detection of HTLV-1–specific HLA-A*24:02-restricted CTLs. Splenocytes from HTLV-1–infected mice at 8 wpi were stained with human CD8 and Tax301-309 tetramer or HIV-1 env gp160 tetramer as a negative control, respectively. Representative results of tetramer-positive CD8 T cells in vivo (left) and ex vivo culture with Tax peptide (right) are shown. (B) Inverse correlation between PVL and the frequency of Tax301-309–specific CTLs. The percentages of tetramer-positive CD8 T cells and PVL in the spleens of 18 HTLV-1–infected mice are shown. One dot represents the result of an individual HTLV-1–infected mouse. Spearman's rank-correlation coefficient (r^2) was used to identify statistically significant correlations. (C) HTLV-1–specific antibody responses in HTLV-1–infected mice. HTLV-1–specific antibody titers in plasma were monitored by the particle agglutination method. Each bar represents an individual mouse. The plasma of indicated mice prior to infection were used as negative-controls (shown as 0 wpi), and these titers were undetectable level (<16). Mice with daggers (mouse ID: X207 and X214) showed biphasic induction of antibody responses; titers peaked at 8 wpi. (D) Detection of HTLV-1–specific IgM or IgG antibody. Antibody depletion was performed by addition of goat antibodies against human IgG or IgM and anti-goat antibody conjugated magnetic beads to the plasma of two mice, as shown in panel C (indicated by daggers). Bars represent antibody titers in the individual X207 and X214 mice. Ab, antibody.

novel preclinical therapies that target viral gene products or cellular molecules critical for viral replication as well as evaluate the efficacy of vaccine candidates to prevent viral expansion in vivo.

Acknowledgments

The authors thank Drs R. Tatsumi and Y. Adachi for advice in establishing humanized mice and assistance with the pathological analysis, respectively. The authors are grateful to the Japanese Red Cross Kinki Cord Blood Bank for providing the samples used in this study.

This work was supported by Grants-in-Aid for Scientific Research C from the Ministry of Education, Culture, Sports, Science and Technology of Japan (grants 21590515 and 24590562) (J.F.); a MEXT-Supported Program for the Strategic Research Foundation at Private Universities; and Health and Labour Sciences Research Grants for Research on Emerging and Re-emerging Infectious Diseases from Ministry of Health, Labour and Welfare (grant 24171601) (T.U.) (grant 23211801) (M. Tanaka).

Authorship

Contribution: K.T. and J.F. designed the research; K.T. and R.X. established and maintained humanized mice; K.T., R.X., M. Tei and T.U. carried out experiments; M. Tanaka was involved in the IL-PCR analysis; K.T., R.X., M. Tei, and J.F. analyzed results; N.T. performed statistical analysis; K.T. designed the figures; and K.T. and J.F. wrote the paper.

Conflict-of-interest disclosure: The authors declare no competing financial interests.

Correspondence: Jun-ichi Fujisawa, Department of Microbiology, Kansai Medical University, 2-5-1 Shin-machi, Hirakata, Osaka 573-1010, Japan; e-mail: fujisawa@hirakata.kmu.ac.jp.

References

1. Hinuma Y, Nagata K, Hanaoka M, et al. Adult T-cell leukemia: antigen in an ATL cell line and detection of antibodies to the antigen in human sera. *Proc Natl Acad Sci USA.* 1981;78(10):6476-6480.
2. Poiesz BJ, Ruscetti FW, Gazdar AF, Bunn PA, Minna JD, Gallo RC. Detection and isolation of type C retrovirus particles from fresh and cultured lymphocytes of a patient with cutaneous T-cell lymphoma. *Proc Natl Acad Sci USA.* 1980;77(12):7415-7419.
3. Osame M, Usuku K, Izumo S, et al. HTLV-I associated myelopathy, a new clinical entity. *Lancet.* 1986;1(8488):1031-1032.
4. Kondo T, Kono H, Miyamoto N, et al. Age- and sex-specific cumulative rate and risk of ATLL for HTLV-I carriers. *Int J Cancer.* 1989;43(6):1061-1064.
5. Boxus M, Twizere JC, Legros S, Dewulf JF, Kettmann R, Willems L. The HTLV-1 Tax interactome. *Retrovirology.* 2008;5:76.
6. Matsuoka M, Jeang KT. Human T-cell leukemia virus type 1 (HTLV-1) and leukemic transformation: viral infectivity, Tax, HBZ and therapy. *Oncogene.* 2011;30(12):1379-1389.
7. Yoshida M, Seiki M, Yamaguchi K, Takatsuki K. Monoclonal integration of human T-cell leukemia provirus in all primary tumors of adult T-cell leukemia suggests causative role of human T-cell leukemia virus in the disease. *Proc Natl Acad Sci USA.* 1984;81(8):2534-2537.
8. Shimoyama M, Minato K, Tobinai K, et al. Atypical adult T-cell leukemia-lymphoma: diverse clinical manifestations of adult T-cell leukemia-lymphoma. *Jpn J Clin Oncol.* 1983;13(Suppl 2):165-187.
9. Okayama A, Tachibana N, Ishihara S, et al. Increased expression of interleukin-2 receptor alpha on peripheral blood mononuclear cells in HTLV-I tax/rex mRNA-positive asymptomatic carriers. *J Acquir Immune Defic Syndr Hum Retrovirol.* 1997;15(1):70-75.

10. Bieberich CJ, King CM, Tinkle BT, Jay G. A transgenic model of transactivation by the Tax protein of HTLV-I. *Virology.* 1993;196(1):309-318.
11. Feuer G, Zack JA, Harrington WJ Jr, et al. Establishment of human T-cell leukemia virus type I T-cell lymphomas in severe combined immunodeficient mice. *Blood.* 1993;82(3): 722-731.
12. Kondo A, Imada K, Hattori T, et al. A model of in vivo cell proliferation of adult T-cell leukemia. *Blood.* 1993;82(8):2501-2509.
13. Furuta RA, Sugiura K, Kawakita S, Inada T, Ikehara S, Matsuda T, Fujisawa J. Mouse model for the equilibration interaction between the host immune system and human T-cell leukemia virus type 1 gene expression. *J Virol.* 2002;76(6): 2703-2713.
14. Dewan MZ, Terashima K, Taruishi M, et al. Rapid tumor formation of human T-cell leukemia virus type 1-infected cell lines in novel NOD-SCID/ gammac(null) mice: suppression by an inhibitor against NF-kappaB. *J Virol.* 2003;77(9): 5286-5294.
15. Hasegawa H, Sawa H, Lewis MJ, et al. Thymus-derived leukemia-lymphoma in mice transgenic for the Tax gene of human T-lymphotropic virus type I. *Nat Med.* 2006;12(4):466-472.
16. Banerjee P, Tripp A, Lairmore MD, et al. Adult T-cell leukemia/lymphoma development in HTLV-1-infected humanized SCID mice. *Blood.* 2010;115(13):2640-2648.
17. Villaudy J, Wencker M, Gadot N, et al. HTLV-1 propels thymic human T cell development in "human immune system" Rag2$^{-/-}$ gamma c$^{-/-}$ mice. *PLoS Pathog.* 2011;7(9):e1002231.
18. Satou Y, Yasunaga J, Zhao T, et al. HTLV-1 bZIP factor induces T-cell lymphoma and systemic inflammation in vivo. *PLoS Pathog.* 2011;7(2): e1001274.
19. Kazanji M. HTLV type 1 infection in squirrel monkeys (Saimiri sciureus): a promising animal model for HTLV type 1 human infection. *AIDS Res Hum Retroviruses.* 2000;16(16):1741-1746.
20. Lairmore MD, Silverman L, Ratner L. Animal models for human T-lymphotropic virus type 1 (HTLV-1) infection and transformation. *Oncogene.* 2005;24(39):6005-6015.
21. Watanabe S, Terashima K, Ohta S, et al. Hematopoietic stem cell-engrafted NOD/SCID/ IL2Rgamma null mice develop human lymphoid systems and induce long-lasting HIV-1 infection with specific humoral immune responses. *Blood.* 2007;109(1):212-218.
22. Yajima M, Imadome K, Nakagawa A, et al. A new humanized mouse model of Epstein-Barr virus infection that reproduces persistent infection, lymphoproliferative disorder, and cell-mediated and humoral immune responses. *J Infect Dis.* 2008;198(5):673-682.
23. Hasegawa A, Ohashi T, Hanabuchi S, Kato H, Takemura F, Masuda T, Kannagi M. Expansion of human T-cell leukemia virus type 1 (HTLV-1) reservoir in orally infected rats: inverse correlation with HTLV-1-specific cellular immune response. *J Virol.* 2003;77(5):2956-2963.
24. Kannagi M, Hasegawa A, Kinpara S, Shimizu Y, Takamori A, Utsunomiya A. Double control systems for human T-cell leukemia virus type 1 by innate and acquired immunity. *Cancer Sci.* 2011; 102(4):670-676.
25. Ito M, Hiramatsu H, Kobayashi K, et al. NOD/SCID/gamma(c)(null) mouse: an excellent recipient mouse model for engraftment of human cells. *Blood.* 2002;100(9):3175-3182.
26. Kushida T, Inaba M, Hisha H, et al. Intra-bone marrow injection of allogeneic bone marrow cells: a powerful new strategy for treatment of intractable autoimmune diseases in MRL/lpr mice. *Blood.* 2001;97(10):3292-3299.
27. Wang J, Kimura T, Asada R, et al. SCID-repopulating cell activity of human cord blood-derived CD34- cells assured by intra-bone marrow injection. *Blood.* 2003;101(8):2924-2931.
28. Miyoshi I, Kubonishi I, Yoshimoto S, et al. Type C virus particles in a cord T-cell line derived by co-cultivating normal human cord leukocytes and human leukaemic T cells. *Nature.* 1981; 294(5843):770-771.
29. Nie C, Sato K, Misawa N, et al. Selective infection of CD4+ effector memory T lymphocytes leads to preferential depletion of memory T lymphocytes in R5 HIV-1-infected humanized NOD/SCID/IL-2Rgammanull mice. *Virology.* 2009;394(1):64-72.
30. Takamori A, Hasegawa A, Utsunomiya A, et al. Functional impairment of Tax-specific but not cytomegalovirus-specific CD8+ T lymphocytes in a minor population of asymptomatic human T-cell leukemia virus type 1-carriers. *Retrovirology.* 2011;8:100.
31. Ueno S, Umeki K, Takajo I, et al. Proviral loads of human T-lymphotropic virus Type 1 in asymptomatic carriers with different infection routes. *Int J Cancer.* 2012;130(10):2318-2326.
32. Etoh K, Tamiya S, Yamaguchi K, et al. Persistent clonal proliferation of human T-lymphotropic virus type I-infected cells in vivo. *Cancer Res.* 1997; 57(21):4862-4867.
33. Umeki K, Hisada M, Maloney EM, Hanchard B, Okayama A. Proviral loads and clonal expansion of HTLV-1-infected cells following vertical transmission: a 10-year follow-up of children in Jamaica. *Intervirology.* 2009;52(3):115-122.
34. Hiramatsu H, Nishikomori R, Heike T, Ito M, Kobayashi K, Katamura K, Nakahata T. Complete reconstitution of human lymphocytes from cord blood CD34+ cells using the NOD/SCID/ gammacnull mice model. *Blood.* 2003;102(3): 873-880.
35. Nitta T, Tanaka M, Sun B, Hanai S, Miwa M. The genetic background as a determinant of human T-cell leukemia virus type 1 proviral load. *Biochem Biophys Res Commun.* 2003;309(1):161-165.
36. Yamano Y, Araya N, Sato T, et al. Abnormally high levels of virus-infected IFN-gamma+ CCR4+ CD4+ CD25+ T cells in a retrovirus-associated neuroinflammatory disorder. *PLoS ONE.* 2009;4(8):e6517.
37. Matsuda M, Maeda Y, Shirakawa C, et al. CD3 down-regulating factor in sera and culture supernatants of leukaemic cells from patients with adult T cell leukaemia. *Br J Haematol.* 1993;83(2): 212-217.
38. Yamada Y, Ohmoto Y, Hata T, et al. Features of the cytokines secreted by adult T cell leukemia (ATL) cells. *Leuk Lymphoma.* 1996;21(5-6): 443-447.
39. Chiba K, Hashino S, Izumiyama K, Toyoshima N, Suzuki S, Kurosawa M, Asaka M. Multiple osteolytic bone lesions with high serum levels of interleukin-6 and CCL chemokines in a patient with adult T cell leukemia. *Int J Lab Hematol.* 2009;31(3):368-371.
40. Chen J, Petrus M, Bryant BR, et al. Autocrine/ paracrine cytokine stimulation of leukemic cell proliferation in smoldering and chronic adult T-cell leukemia. *Blood.* 2010;116(26):5948-5956.
41. Ohshima K, Mukai Y, Shiraki H, Suzumiya J, Tashiro K, Kikuchi M. Clonal integration and expression of human T-cell lymphotropic virus type I in carriers detected by polymerase chain reaction and inverse PCR. *Am J Hematol.* 1997; 54(4):306-312.
42. Kurihara K, Harashima N, Hanabuchi S, et al. Potential immunogenicity of adult T cell leukemia cells in vivo. *Int J Cancer.* 2005;114(2):257-267.
43. Akimoto M, Kozako T, Sawada T, et al. Anti-HTLV-1 tax antibody and tax-specific cytotoxic T lymphocyte are associated with a reduction in HTLV-1 proviral load in asymptomatic carriers. *J Med Virol.* 2007;79(7):977-986.
44. Harashima N, Kurihara K, Utsunomiya A, et al. Graft-versus-Tax response in adult T-cell leukemia patients after hematopoietic stem cell transplantation. *Cancer Res.* 2004;64(1):391-399.
45. Kozako T, Arima N, Toji S, et al. Reduced frequency, diversity, and function of human T cell leukemia virus type 1-specific CD8+ T cell in adult T cell leukemia patients. *J Immunol.* 2006; 177(8):5718-5726.
46. Nakamura K, Inaba M, Sugiura K, Yoshimura T, Kwon AH, Kamiyama Y, Ikehara S. Enhancement of allogeneic hematopoietic stem cell engraftment and prevention of GVHD by intra-bone marrow bone marrow transplantation plus donor lymphocyte infusion. *Stem Cells.* 2004; 22(2):125-134.
47. Jaatinen T, Hemmoranta H, Hautaniemi S, et al. Global gene expression profile of human cord blood-derived CD133+ cells. *Stem Cells.* 2006; 24(3):631-641.
48. Herrera MB, Bruno S, Buttiglieri S, et al. Isolation and characterization of a stem cell population from adult human liver. *Stem Cells.* 2006;24(12): 2840-2850.
49. Martin-Rendon E, Hale SJ, Ryan D, et al. Transcriptional profiling of human cord blood CD133+ and cultured bone marrow mesenchymal stem cells in response to hypoxia. *Stem Cells.* 2007;25(4):1003-1012.
50. Kuruvilla JG, Troyer RM, Devi S, Akkina R. Dengue virus infection and immune response in humanized RAG2($^{-/-}$)gamma(c)($^{-/-}$) (RAG-hu) mice. *Virology.* 2007;369(1):143-152.

INTERNAL MEDICINE

□ ORIGINAL ARTICLE □

Cerebrospinal Fluid Neopterin, but not Osteopontin, is a Valuable Biomarker for the Treatment Response in Patients with HTLV-I-associated Myelopathy

Masahiro Nagai, Tomoaki Tsujii, Hirotaka Iwaki, Noriko Nishikawa and Masahiro Nomoto

Abstract

Objective The concentrations of neopterin and osteopontin in the cerebrospinal fluid (CSF) were measured in patients with HTLV-I-associated myelopathy/tropical spastic paraparesis (HAM/TSP) in order to evaluate their utility as biomarkers for the treatment response.

Methods Seven HAM/TSP patients were treated intravenously with high-dose methylprednisolone (1,000 mg/day) for 3 days. CSF samples were collected before and after the treatment. The neopterin and osteopontin concentrations were determined using high-performance liquid chromatography (HPLC) and an enzyme immunoassay, respectively. The clinical symptoms were evaluated using the Osame Motor Disability Score and the Urinary Disturbance Score.

Results Four out of the seven patients showed an improvement in motor function with the treatment, and were therefore classed as responders. The pre-treatment CSF neopterin concentration exceeded the upper limit of normal in all seven of the patients, and tended to be higher in treatment responders as compared to non-responders. The CSF neopterin concentration was reduced following treatment in all patients. The mean CSF neopterin concentration significantly ($p<0.01$) decreased following treatment by almost 60% (from 124.1±79.9 nmol/L to 49.2±29.8 nmol/L). The mean CSF osteopontin concentration was significantly ($p<0.01$) higher in the HAM/TSP patients in comparison to the 18 HTLV-1-seronegative patients who were designated as controls (9.54±4.53 mg/L vs. 3.72±3.04 mg/L). No significant ($p=0.47$) reduction of the CSF osteopontin concentration was observed following the intravenous administration of high-dose methylprednisolone.

Conclusion These results indicate that the CSF neopterin concentration, but not the osteopontin concentration, is a potentially valuable biomarker for monitoring the treatment response in HAM/TSP patients. Furthermore, high pre-treatment CSF neopterin concentrations may be a predictive biomarker for a response to intravenous high-dose methylprednisolone therapy.

Key words: HTLV-I, HAM/TSP, cerebrospinal fluid, neopterin, osteopontin, methylprednisolone

(Intern Med 52: 2203-2208, 2013)
(DOI: 10.2169/internalmedicine.52.0869)

Introduction

Human T-cell lymphotropic virus type I (HTLV-I) is an exogenous human retrovirus that has been demonstrated to be the etiological agent in adult T-cell leukemia as well as in a progressive neurological disease called HTLV-I-associated myelopathy/tropical spastic paraparesis (HAM/TSP). The vast majority of HTLV-I-infected individuals are clinically asymptomatic, with <5% of infected individuals ever developing HAM/TSP. Clinically, HAM/TSP is characterized by muscle weakness, hyperreflexia, spasticity in the lower extremities and urinary disturbance associated with the preferential damage of the thoracic spinal cord (1). Although it is not yet completely understood how HTLV-I causes HAM/TSP, it is believed that increased HTLV-I

Department of Neurology and Clinical Pharmacology, Ehime University Graduate School of Medicine, Japan
Received for publication April 26, 2013; Accepted for publication June 2, 2013
Correspondence to Dr. Masahiro Nomoto, nomoto@m.ehime-u.ac.jp

Table 1. Patient Characteristics

Patient no.	Age (years)	Sex	Disease duration (years)	CSF anti-HTLV-I antibody titer
1	70	M	13	1:512
2	81	F	2	1:800
3	48	F	2	1:256
4	48	F	4	1:800
5	77	F	5	1:512
6	60	F	2	1:512
7	56	F	10	1:128

F: female, M: male

Table 2. Rating Scale for the Osame Motor Disability Score

0	Normal walking and running
1	Normal gait but runs slowly
2	Abnormal gait
3	Abnormal gait and unable to run
4	Needs support while using stairs
5	Needs 1-hand support in walking
6	Needs 2-hand support in walking
7	Needs 2-hand support in walking and is limited to 10 m
8	Needs 2-hand support in walking and is limited to 5 m
9	Unable to walk but able to crawl on hands and knees
10	Crawls with hands
11	Unable to crawl but can turn sideways in bed
12	Unable to turn sideways but can move toes
13	Completely bedridden

proviral loads and immune responses to HTLV-I infected cells play a pivotal role in the pathogenesis of this disorder (2).

Consequently, therapeutic strategies for HAM/TSP patients are directed towards these pathogenic phenomena. The first therapeutic strategy is to reduce HTLV-I loads, although anti-retroviral reagents such as reverse transcriptase inhibitors seem to be less effective for HTLV-I infections than for human immunodeficiency virus (HIV) infections. The second therapeutic strategy is to modulate the abnormal immune responses in HAM/TSP patients. Several immunosuppressive or immunomodulating therapies have been tried, including corticosteroids, interferon-α (IFN-α), azathioprine and plasmapheresis (3). Chronic oral prednisolone therapy was empirically the most effective for the improvement the neurological impairment that is associated with HAM/TSP. However, adverse events such as osteoporosis, glucose intolerance and gastroduodenal ulceration have limited its use for HAM/TSP patients, especially elderly postmenopausal women. We have chosen IV high-dose methylprednisolone as a first-line therapy because this treatment has a better tolerability profile than chronic oral prednisolone therapy. Another reason is because IV high-dose methylprednisolone therapy has been extensively and successfully used for patients with relapses of multiple sclerosis or other immune-mediated neurological disorders.

Although the anti-HTLV-I antibody titer in the cerebrospinal fluid (CSF) is used as a diagnostic biomarker of HAM/TSP, it is inadequate as a biomarker for monitoring the treatment response. However, increased CSF neopterin concentrations have been previously reported in patients with HAM/TSP (4, 5). Neopterin is a pyrazino-pyrimidine compound that is produced by macrophages after stimulation by IFN-γ from activated T cells. The concentration of neopterin in the CSF has been used as a biomarker for cellular immune response in the central nervous system (CNS). Osteopontin has multiple functions and is involved in the recruitment of macrophage and T cells in inflammatory lesions. Osteopontin enhances IFN-γ and interleukin (IL)-12 production and depresses the release of IL-10 from immune cells (6). It is up-regulated in the brains of patients with multiple sclerosis and in the spinal cords of mice with experimental autoimmune encephalomyelitis (7, 8). It is therefore believed that both neopterin and osteopontin could be valuable biomarkers for indicating the severity of inflammation and the degree of T cell activation in the CNS.

Chronic oral prednisolone therapy decreases CSF neopterin concentrations in HAM/TSP patients (3). However, it is not yet known if CSF neopterin concentrations change rapidly after treatment and might, therefore, be useful in predicting the response to corticosteroid therapy. The CSF osteopontin concentrations in HAM/TSP patients have not yet been investigated. We herein present the results of our study in which we monitored the CSF neopterin and osteopontin concentrations before and after IV high-dose methylprednisolone therapy in patients with HAM/TSP in order to evaluate their utility as biomarkers for treatment response.

Materials and Methods

The diagnosis of HAM/TSP was made according to the current WHO diagnosis guidelines. The anti-HTLV-I antibody titers were measured using a particle-agglutination (PA) test. The characteristics of the seven patients with HAM/TSP who were recruited are summarized in Table 1. They had not been previously treated with either immunosuppressive or immunomodulating agents. They were treated with IV infusions of high-dose methylprednisolone (1,000 mg/day) for 3 days following their hospital admission. None of the patients received any additional oral corticosteroid therapy following the IV administration of high-dose methylprednisolone. The Osame Motor Disability Score (OMDS) and the Urinary Disturbance Score (UDS) were used for the clinical evaluation. The OMDS rating scale is shown in Table 2. The UDS was calculated from the sum of the scores (0=normal, 1=slight, 2=moderate, 3=severe) for three symptoms (increased frequency of urination, feeling of residual urine, incontinence). CSF was obtained from each patient with written informed consent. Lumbar punctures were performed before and within 7 days of treatment completion. The collected CSF was stored at -80℃ until analyzed. The study was approved by the hospital ethics committee.

The CSF neopterin concentrations were measured using high-performance liquid chromatography (HPLC) with fluorometric detection. Thawed CSF aliquots (100 μL) were acidified with ice-cold 0.1 M HCl (100 μL) and kept on ice.

A mixture of 1% I_2 and 2% KI in 0.1 M HCl (50 μL) was then added, and the samples were incubated at room temperature under dark conditions. An aqueous solution of 1.5% ascorbic acid (50 μL) was then added to the mixture, which was then centrifuged at 10,000 rpm for 1 min. The supernatant (100 μL) was injected into a C18 column (150× 2.1 mm) with 3.5% methanol in water as the mobile phase. The quantification of osteopontin in the CSF samples was performed using a commercially available enzyme immunoassay kit (human osteopontin assay kit, Immuno-Biological Laboratories, Japan) according to the manufacturer's protocol.

Statistical analysis was performed using the JMP10 software program (SAS). The results are expressed as mean±SD and median values. The paired data from before and after treatment were analyzed by Wilcoxon's signed-rank test. The Mann-Whitney U test was used to compare groups. p values of <0.05 were considered to be statistically significant.

Results

Four out of the seven patients showed improvement in their motor function after treatment with IV high-dose methylprednisolone. One patient improved by two grades and the others improved by one grade on the OMDS rating scale (Table 3). An improvement in the urinary disturbance score was observed in four patients (Table 3). Three of the patients showed improvements on both scales, while one patient showed an improvement in the urinary disturbance score without an associated improvement in motor function and a second patient showed improved motor function without an improvement in the urinary disturbance score. Five patients had sensory disturbance (pain and numbness of lower limbs and back pain) before the treatment. The treatment alleviated pain in all five patients.

The CSF neopterin concentrations exceeded the upper limit of normal (30 nmol/L) in all of the patients before treatment. The mean CSF neopterin concentration was 124.1±79.9 nmol/L (median 89.9 nmol/L) for all seven patients prior to treatment. The CSF neopterin concentrations decreased in all of the patients after IV high-dose methylprednisolone therapy. The mean CSF neopterin concentration was significantly ($p<0.01$) reduced by almost 60% after treatment to 49.2±29.8 nmol/L (median: 43.4 nmol/L) (Table 4). The changes in the CSF neopterin concentrations according to the treatment parameters for each patient are shown in Fig. 1.

Table 3. Changes in the Disability Scores after IV High-dose Methylprednisolone Therapy

Patient no.	OMDS		UDS	
	Before	After	Before	After
1	5	4	6	5
2	10	8	9	7
3	4	4	5	3
4	3	3	3	3
5	5	4	3	3
6	10	9	7	6
7	5	5	3	3

OMDS: Osame Motor Disability Score, UDS: Urinary Disturbance Score

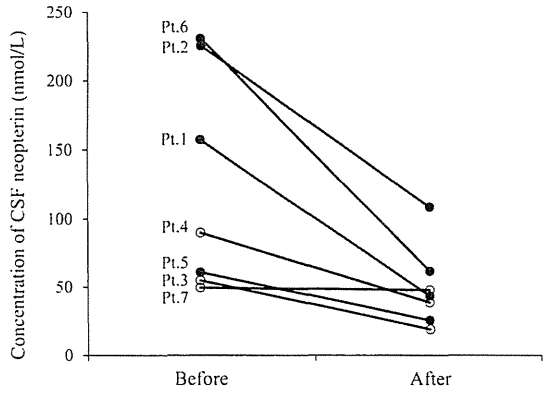

Figure 1. The CSF neopterin concentrations before and after IV high-dose methylprednisolone therapy. The closed and open symbols indicate clinical responders and non-responders, respectively.

Table 4. Changes in the CSF Parameters after IV High-dose Methylprednisolone Therapy

Patient no.	Neopterin (nmol/L)		Osteopontin (mg/L)		anti-HTLV-I antibody titer		Cells (/μL)		Protein (mg/dL)	
	Before	After	Before	After	Before	After	Before	After	Before	After
1	157.4	43.4	10.69	13.46	1:512	1:512	6	2	25	27
2	225.5	108.7	7.22	9.36	1:800	1:256	10	8	54	50
3	54.9	18.9	3.67	5.05	1:256	1:128	6	7	45	29
4	89.9	38.5	13.15	12.33	1:800	1:800	7	6	50	44
5	60.9	25.4	4.66	4.81	1:512	1:128	3	3	39	35
6	230.8	61.7	16.02	11.50	1:512	1:512	12	6	52	29
7	49.5	47.8	11.36	3.70	1:128	1:256	5	7	20	23

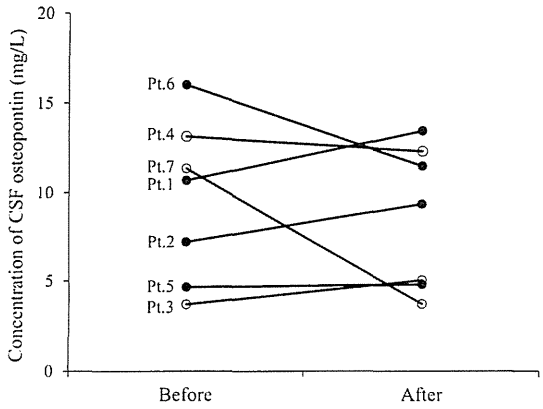

Figure 2. The CSF osteopontin concentrations before and after IV high-dose methylprednisolone therapy. The closed and open symbols indicate clinical responders and non-responders, respectively.

The mean CSF osteopontin concentration was 9.54±4.53 mg/L (median 10.69 mg/L) prior to treatment. Unlike for neopterin, our laboratory had not yet set an upper limit of normal for CSF osteopontin. We therefore compared CSF osteopontin concentrations for our seven HAM/TSP patients to those for 18 HTLV-I-seronegative patients with spondylosis as a control group. The mean CSF osteopontin concentration was 3.72±3.04 mg/L (median 3.52 mg/L) in the control group. The pre-treatment CSF osteopontin concentration in our seven HAM/TSP patients was significantly ($p<0.01$) higher than that of the control group. The mean CSF osteopontin concentration was 8.6±4.03 mg/L (median: 9.36 mg/L) after treatment in the seven HAM/TSP patients, which was not significantly ($p=0.47$) different than the pre-treatment values (Table 4). The pre-treatment and post-treatment CSF osteopontin concentrations for each HAM/TSP patient are shown in Fig. 2.

We defined HAM/TSP patients who showed an OMDS improvement as responders. The mean pre-treatment CSF neopterin concentration in responders (n=4) was 168.7±79.2 nmol/L (median 191.5 nmol/L), but only 64.8±22.0 nmol/L (median 54.9 nmol/L) in non-responders (n=3). While the pre-treatment CSF neopterin concentrations tended to be higher among responders compared to non-responders, the difference was not statistically significant ($p=0.056$). The mean pre-treatment CSF osteopontin concentration was 9.64±4.91 mg/L (median 8.95 mg/L) in responders and 9.34±5.04 mg/L (median 11.36 mg/L) in non-responders with no significant difference between the groups ($p=0.43$).

The HTLV-I antibody titer, and the number of cells and the amount of protein in the CSF were not significantly altered by the treatment (Table 4).

The IV high-dose methylprednisolone therapy was well tolerated by all of the patients. Although insomnia was observed as an adverse effect of treatment, it was transient. No serious adverse events were observed.

Discussion

We herein demonstrate that the CSF neopterin concentration significantly decreases following IV high-dose methylprednisolone therapy in patients with HAM/TSP. While the pre-treatment CSF osteopontin concentrations were significantly higher in HAM/TSP patients as compared to the controls, there were no statistically significant changes in the CSF osteopontin concentrations after treatment.

The coexistence of a high HTLV-I proviral load and HTLV-I-specific T cells is an important feature of HAM/TSP (9). This distinguishing feature is observed in both peripheral blood and CSF of patients with HAM/TSP (9, 10). Histopathological studies indicate the existence of HTLV-I-infected cells as well as a local inflammatory response in the spinal cord lesions of HAM/TSP patients (11, 12). It is therefore believed that the immune response to HTLV-I likely contributes to the inflammatory process of the CNS lesions in HAM/TSP patients and causes the clinical symptoms of HAM/TSP. Activated lymphocytes and macrophages up-regulate the production of pro-inflammatory cytokines such as IL-1, IL-6 and IFN-γ (13). The significant elevation of the levels of these cytokines has been described in the CSF of HAM/TSP patients (14, 15). High values of CSF neopterin have also been reported in HAM/TSP patients (4, 5). Neopterin is released by stimulated macrophages, and the concentration of CSF neopterin reflects the degree of the inflammatory response in the CNS. The concentration of CSF neopterin is significantly correlated with the HTLV-I proviral load, which is an important risk factor for the development of HAM/TSP (10). The CSF neopterin concentration is therefore useful as an adjunct to the diagnosis of HAM/TSP. In our study, we confirmed the elevation of CSF neopterin concentrations in HAM/TSP patients.

Moreover, we also demonstrated that CSF osteopontin concentrations are increased in HAM/TSP patients. To the best of our knowledge, this is the first report concerning osteopontin concentrations in HAM/TSP patients. Osteopontin is a secreted phosphoprotein that is produced by many kinds of cells including osteoblasts, activated lymphocytes, macrophages, vascular smooth muscle cells and kidney cells (16). It has a multifunctional capacity, and is involved in bone remodeling, tumor progression, atherosclerosis, inflammation and immunity (16). Osteopontin promotes the production of pro-inflammatory cytokines such as IL-12 and IFN-γ (6). Several studies have reported that osteopontin concentrations are significantly elevated in the CSF of patients with multiple sclerosis (17-19). Our finding suggests that a chronic inflammatory response in the CNS lesions of HAM/TSP is reflected by the CSF osteopontin concentrations as well as the CSF neopterin concentrations. If so, which is the better diagnostic marker for HAM/TSP? The CSF neopterin concentrations exceeded the upper limit of normal in all HAM/TSP patients. However, the CSF osteopontin concentrations in three of the seven HAM/TSP patients overlapped the range

measured for the control group. Thus, the CSF neopterin concentration would appear to be more suitable for discriminating HAM/TSP and non-HAM/TSP patients than CSF osteopontin concentration.

Various treatments have been tried for HAM/TSP patients (3). Almost all of the studies have been open-label trials or case series with the exception of a multicenter, randomized placebo-controlled, double-blind study of an IFN-α trial in Japan (20). However, no study has conclusively demonstrated a long-term clinical benefit. Well-designed clinical trials are therefore necessary in order to develop effective therapies which may improve the long-term prognoses for HAM/TSP patients (21). In addition, validated surrogate biomarkers are required for the determination of the effectiveness of investigational treatments.

It has been previously reported that approximately 70% of HAM/TSP patients who are treated with a chronic oral administration of prednisolone (n=131) improved by at least one OMDS grade (3). Furthermore, the treatment significantly decreased the reported CSF neopterin concentrations in 16 patients. The mean CSF neopterin concentration was also reduced from 155.4 nmol/L to 79.5 nmol/L by IV high-dose methylprednisolone therapy in eight of the previously reported patients, but the change was not statistically significant (3). Unfortunately, the timing of the CSF sampling after IV high-dose methylprednisolone therapy was not specified in that publication. The timing of CSF sampling is likely critical with such short-term therapies as IV high-dose methylprednisolone, since the CSF neopterin concentration seems to increase after the discontinuation of treatment. In our study, the CSF samples were collected within 7 days of the completion of the IV high-dose methylprednisolone therapy in order to attenuate the impact of the change on the CSF neopterin concentration. The CSF neopterin concentration changed rapidly after IV high-dose methylprednisolone therapy. This finding suggests that CSF neopterin is a sensitive biomarker for the evaluation of the early-phase response to treatments in HAM/TSP patients. This feature may be partially due to the short half-life of neopterin which has been estimated to be 90 minutes in the circulation (22). In contrast, there was no significant change in the CSF osteopontin concentrations that were was observed after IV high-dose methylprednisolone therapy in the HAM/TSP patients. Even though there is a possibility that a change in the CSF osteopontin concentration may arise several days after the treatment, it is clear that the CSF osteopontin concentration is unreliable as a biomarker for the assessment of an early-phase response to treatment. Although the influence of IV high-dose methylprednisolone therapy on HTLV-I proviral loads is still unclear, the therapy doesn't seem to reduce HTLV-I proviral loads. It has been reported that the osteopontin gene was transactivated by HTLV-I Tax protein (23). If the elevation of the CSF osteopontin levels in HAM/TSP patients is due to an HTLV-I infection of the osteopontin producing cells, but not the inflammatory response, then the unchanged osteopontin levels by IV high-dose methylprednisolone therapy are thus thought to be understandable.

Although it was not a statistically significant difference, and it is most likely due to the small number of patients, the pre-treatment CSF neopterin concentrations of those patients who responded to the IV high-dose methylprednisolone therapy tended to be higher than those of non-responders. This suggests that patients with relatively high values of CSF neopterin may have a more favorable response to IV high-dose methylprednisolone therapy. Additional patients need to be examined in order to confirm the belief that CSF neopterin is useful as a predictive biomarker for responders to IV high-dose methylprednisolone therapy.

The mechanism of action of for the corticosteroids on HAM/TSP remains to be elucidated. The anti-inflammatory properties of the corticosteroids may attenuate the degree of the inflammatory response in spinal cord lesions. This non-specific anti-inflammatory effect may result in clinical improvements in the patients, especially when the inflammation is very intense. Moreover, corticosteroids may also affect the HTLV-I infected cells or the immune response to HTLV-I. It has been demonstrated that betamethasone therapy decreased $CD4^+Tax^+$ T cells and increased $CD4^+Foxp3^+$ T cells (regulatory T cells) in the peripheral blood samples of patients with HAM/TSP (24). Corticosteroids therapy may reduce the erratic IFN-γ production by T-cells in patients with HAM/TSP, which is then followed by a reduction of neopterin release by the stimulated macrophages.

Our study did not address how long the clinical effect and the reduction of CSF neopterin concentration lasted after the IV high-dose methylprednisolone therapy had been discontinued. An open-label clinical trial of IV high-dose methylprednisolone has been reported from Brazil, in which 39 patients with HAM/TSP received IV high-dose methylprednisolone every 3-4 months (25). The Incapacity Status Scale showed a significant neurological improvement of 24.5% after a mean follow-up of 2.2 years. However, the CSF biomarkers were not reported in that trial. Further study will therefore be needed to clarify the long-term changes in the CSF neopterin concentration following the treatment of HAM/TSP patients.

In conclusion, our results indicate that the concentration of CSF neopterin, but not that of osteopontin, is a potentially valuable biomarker for monitoring treatment response in HAM/TSP patients. In addition, high pre-treatment CSF neopterin concentrations may be a predictive biomarker for response to IV high-dose methylprednisolone therapy.

The authors state that they have no Conflict of Interest (COI).

Acknowledgement

This study was supported by Grant-in-Aids for Orphan and Neurodegenerative Disorders from the Ministry of Health, Labour and Welfare, GJTS, and a Grant of Ehime University. The authors wish to thank Ms. Madoka Kubo for her excellent technical assistance.

References

1. Osame M, Usuku K, Izumo S, et al. HTLV-I associated myelopathy, a new clinical entity. Lancet **1**: 1031-1032, 1986.
2. Nagai M, Osame M. Human T-cell lymphotropic virus type I and neurological diseases. J Neurovirol **9**: 228-235, 2003.
3. Nakagawa M, Nakahara K, Maruyama Y, et al. Therapeutic trials in 200 patients with HTLV-I-associated myelopathy/tropical spastic paraparesis. J Neurovirol **2**: 345-355, 1996.
4. Nomoto M, Utatsu Y, Soejima Y, Osame M. Neopterin in cerebrospinal fluid: a useful marker for diagnosis of HTLV-I-associated myelopathy/tropical spastic paraparesis. Neurology **41**: 457, 1991.
5. Ali A, Rudge P, Dalgleish AG. Neopterin concentrations in serum and cerebrospinal fluid in HTLV-I infected individuals. J Neurol **239**: 270-272, 1992.
6. Ashkar S, Weber GF, Panoutsakopoulou V, et al. Eta-1 (osteopontin): an early component of type-1 (cell-mediated) immunity. Science **287**: 860-864, 2000.
7. Chabas D, Baranzini SE, Mitchell D, et al. The influence of the proinflammatory cytokine, osteopontin, on autoimmune demyelinating disease. Science **294**: 1731-1735, 2001.
8. Braitch M, Constantinescu CS. The role of osteopontin in experimental autoimmune encephalomyelitis (EAE) and multiple sclerosis (MS). Inflamm Allergy Drug Targets **9**: 249-256, 2010.
9. Nagai M, Yamano Y, Brennan MB, Mora CA, Jacobson S. Increased HTLV-I proviral load and preferential expansion of HTLV-I Tax-specific $CD8^+$ T cells in cerebrospinal fluid from patients with HAM/TSP. Ann Neurol **50**: 807-812, 2001.
10. Nagai M, Usuku K, Matsumoto W, et al. Analysis of HTLV-I proviral load in 202 HAM/TSP patients and 243 asymptomatic HTLV-I carriers: high proviral load strongly predisposes to HAM/TSP. J Neurovirol **4**: 586-593, 1998.
11. Matsuoka E, Takenouchi N, Hashimoto K, et al. Perivascular T cells are infected with HTLV-I in the spinal cord lesions with HTLV-I-associated myelopathy/tropical spastic paraparesis: double staining of immunohistochemistry and polymerase chain reaction in situ hybridization. Acta Neuropathol **96**: 340-346, 1998.
12. Umehara F, Izumo S, Nakagawa M, et al. Immunocytochemical analysis of the cellular infiltrate in the spinal cord lesions in HTLV-I-associated myelopathy. J Neuropathol Exp Neurol **52**: 424-430, 1993.
13. Umehara F, Izumo S, Ronquillo AT, Matsumuro K, Sato E, Osame M. Cytokine expression in the spinal cord lesions in HTLV-I-associated myelopathy. J Neuropathol Exp Neurol **53**: 72-77, 1994.
14. Nishimoto N, Yoshizaki K, Eiraku N, et al. Elevated levels of interleukin-6 in serum and cerebrospinal fluid of HTLV-I-associated myelopathy/tropical spastic paraparesis. J Neurol Sci **97**: 183-193, 1990.
15. Furuya T, Nakamura T, Fujimoto T, et al. Elevated levels of interleukin-12 and interferon-gamma in patients with human T lymphotropic virus type I-associated myelopathy. J Neuroimmunol **95**: 185-189, 1999.
16. Denhardt DT, Guo X. Osteopontin: a protein with diverse functions. FASEB J **7**: 1475-1482, 1993.
17. Braitch M, Nunan R, Niepel G, Edwards LJ, Constantinescu CS. Increased osteopontin levels in the cerebrospinal fluid of patients with multiple sclerosis. Arch Neurol **65**: 633-635, 2008.
18. Bornsen L, Khademi M, Olsson T, Sorensen PS, Sellebjerg F. Osteopontin concentrations are increased in cerebrospinal fluid during attacks of multiple sclerosis. Mult Scler **17**: 32-42, 2011.
19. Wen SR, Liu GJ, Feng RN, et al. Increased levels of IL-23 and osteopontin in serum and cerebrospinal fluid of multiple sclerosis patients. J Neuroimmunol **244**: 94-96, 2012.
20. Izumo S, Goto I, Itoyama Y, et al. Interferon-alpha is effective in HTLV-I-associated myelopathy: a multicenter, randomized, double-blind, controlled trial. Neurology **46**: 1016-1021, 1996.
21. Yamano Y, Sato T. Clinical pathophysiology of human T-lymphotropic virus-type 1-associated myelopathy/tropical spastic paraparesis. Front Microbiol **3**: 389, 2012.
22. Fuchs D, Stahl-Hennig C, Gruber A, et al. Neopterin: its clinical use in urinalysis. Kidney Int Suppl **47**: S8-S11, 1994.
23. Zhang J, Yamada O, Matsushita Y, et al. Transactivation of human osteopontin promoter by human T-cell leukemia virus type 1-encoded Tax protein. Leuk Res **34**: 763-768, 2010.
24. Alberti C, Cartier L, Valenzuela MA, Puente J, Tanaka Y, Ramirez E. Molecular and clinical effects of betamethasone in human T-cell lymphotropic virus type-I-associated myelopathy/tropical spastic paraparesis patients. J Med Virol **83**: 1641-1649, 2011.
25. Croda MG, de Oliveira AC, Vergara MP, et al. Corticosteroid therapy in TSP/HAM patients: the results from a 10 years open cohort. J Neurol Sci **269**: 133-137, 2008.

Journal of Neuroimmunology 254 (2013) 183–186

Contents lists available at SciVerse ScienceDirect

Journal of Neuroimmunology

journal homepage: www.elsevier.com/locate/jneuroim

Short communication

Antibodies against Wnt receptor of muscle-specific tyrosine kinase in myasthenia gravis

Masaharu Takamori [a,*], Tatsufumi Nakamura [b], Masakatsu Motomura [c]

[a] Neurological Center, Kanazawa-Nishi Hospital, 6-15-41, Ekinishi-Honmachi, Kanazawa, Ishikawa-ken 920-0025, Japan
[b] Department of Molecular Microbiology and Immunology, Graduate School of Biomedical Sciences, Nagasaki University, 1-12-4, Sakamoto, Nagasaki, Nagasaki-ken 852-8523, Japan
[c] Department of Internal Medicine, Graduate School of Biomedical Sciences, Nagasaki University, 1-7-1, Sakamoto, Nagasaki, Nagasaki-ken 852-8501, Japan

ARTICLE INFO

Article history:
Received 7 June 2012
Received in revised form 21 July 2012
Accepted 3 September 2012

Keywords:
Myasthenia gravis
Neuromuscular junction
Acetylcholine receptor
Muscle-specific tyrosine kinase
Wnt

ABSTRACT

Muscle-specific tyrosine kinase (MuSK) antibodies are detected in a proportion of myasthenia gravis (MG) patients who are negative for acetylcholine receptor (AChR) antibodies and have prominent bulbar weakness and crises. In the MuSK ectodomains, the immunoglobulin-like 1 and 2 domains (Ig1/2) mediate the agrin–Lrp4–MuSK signaling and the cysteine-rich domain (CRD) mediates the Wnt–MuSK–Dishevelled signaling; both contribute to AChR clustering. Immunoblotting against recombinant proteins showed MuSK Ig1/2 antibodies in 33 anti-AChR-negative MG patients; 10 patients of them (30%) were additionally positive for MuSK CRD antibodies. The result suggests that MuSK antibodies have heterogeneity in their binding to functional domains of MuSK.

1. Introduction

Myasthenia gravis (MG) is a disease of neuromuscular junction (NMJ) which is mainly caused by an immune response to the nicotinic acetylcholine receptor (AChR) in skeletal muscle. A proportion of MG patients are negative for AChR antibodies, and instead have antibodies (largely IgG4 and partially IgG1) against the muscle-specific tyrosine kinase (MuSK) (Vincent et al., 2008) with the clinical features including prevalence in women, prominent bulbar involvement, crises and anticholinesterase nonresponsiveness (Pasnoor et al., 2010; Guptill et al., 2011). MuSK is stimulated from "inside" the muscle cells by Dok7 (Yamanashi et al., 2012), and from the "outside" by Lrp4 (agrin receptor) with and without agrin (Weatherbee et al., 2006; Kim et al., 2008; Zhang et al., 2008); MuSK thereby contributes to AChR stabilization and clustering through various intracellular kinase cascades (Wu et al., 2010). Also, MuSK contains the receptor for Wnts which belong to a family of secreted glycoproteins and interact with the muscle-expressed Dishevelled (Dvl) that is essential for the noncanonical Wnt signaling cascade contributing to AChR clustering (Luo et al., 2002; Korkut and Budnik, 2009; Wu et al., 2010); this pathway also regulates a retrograde signaling to nerve terminals (Luo et al., 2002). In the MuSK ectodomains, its first and second immunoglobulin-like domains (Ig1/2) mediate the agrin–Lrp4 signaling (Stiegler et al., 2006) and its cysteine-rich domain (CRD) mediates the Wnt signaling (Stiegler et al., 2009). In view of these, we studied the MG patients focusing on the antibodies against the MuSK CRD in association with the antibodies against the MuSK Ig1/2 domains.

2. Patients and methods

2.1. Patients

Serum samples were obtained from 43 anti-AChR-negative patients, aged from 6 to 80 years at onset (13 men and 30 women), with generalized MG defined by the Myasthenia Gravis Foundation of America (MGFA) classification (grades from IIa to V) (Jaretzki et al., 2000). The diagnosis was based on fatigable muscle weakness with electrophysiological evidence of decrementing compound muscle action potentials to low-rate repetitive nerve stimulation or increased jitter on single-fiber electromyography; a positive response to edrophonium injection was considered as a finding in favor of the diagnosis. Thirty-three patients, aged from 6 to 80 years at onset (10 men and 23 women), of these 43 patients were positive for MuSK antibodies (ranged from 5.32 to 131.40 nM. control, <0.05 nM) determined by the standard radioimmunoassay (RIA) (McConville et al., 2004); the remaining 10 patients negative for standard RIA-determined MuSK antibodies, aged from 20 to 65 years at onset (3 men and 7 women) were also studied as MG diagnosed by clinical and electrophysiological features (MGFA-graded from IIa to IIIa). Control sera were obtained from 10 healthy volunteers aged from 22 to 43 years (5 men and 5 women) and from 10 disease controls with MG, aged from 18 to 70 years at onset (2 men

* Corresponding author. Tel.: +81 76 233 1811; fax: +81 76 221 8603.
E-mail address: m-takamori@vanilla.ocn.ne.jp (M. Takamori).

0165-5728/$ – see front matter © 2012 Elsevier B.V. All rights reserved.
http://dx.doi.org/10.1016/j.jneuroim.2012.09.001

and 8 women) and MGFA-graded from IIb to IIIb who were positive for AChR antibodies (from 5.6 to 77.0 nM. control, <0.2 nM) and negative for standard RIA-determined MuSK antibodies (<0.05 nM).

2.2. Recombinant expression of MuSK Ig1/2 domains and CRD

DNA fragments coding from human MuSK Ig1/2 domain-contained amino acid residues (22–212) (Stiegler et al., 2006) and CRD-contained amino acid residues (313–494) (Stiegler et al., 2009) were generated by PCR method using human MuSK cDNA (OriGene Technol., USA) as a template. Expression constructs were generated in pcDNA3.3-TOPO (Invitrogen, USA) with DNA fragments ligated to the synthetic mouse trypsin prepro sequence followed by 7 histidines tagged at the N-terminus. Human embryonic kidney (HEK) 293F cells (Invitrogen, USA) were transiently transfected with these constructs according to the instructions (FreeStyle™293 Expression System, Invitrogen, USA), and the cultured supernatants were harvested for 4 days after transfection. Clarified supernatants were directly loaded onto a HisTrap HP column (GE Healthcare, USA) equilibrated with 0.1 M Tris–Cl, 0.5 M NaCl, 20 mM Imidazole, pH 7.4. After the column was washed with the equilibration buffer, Ig1/2 and CRD proteins were eluted with linear gradient of Imidazole. Purity of Ig1/2 and CRD proteins was analyzed by sodium dodecyl sulfate-polyacrylamide gel electrophoresis (SDS-PAGE) (Invitrogen, USA) and Western blotting using mouse anti-human monoclonal antibodies (ab86456 for Ig1/2 and ab55549 for CRD. Abcam, USA).

2.3. Western blot analysis

Either Ig1/2 domains or CRD of MuSK at an amount of 5 μg/lane was subjected to 12.5% SDS-PAGE under reducing conditions with dithiothreitol. Proteins were transfected onto a polyvinylidene difluoride membrane and were then cut into strips. The antibody detection was performed by using Immun-Blot® Assay Kit (Bio-Rad Lab., USA). In brief, after blocking with Tris buffered saline containing 3% gelatin for 1 h, each strip was incubated with the serum sample which was diluted from 1:100 to 1:1000 and with a 1000-fold-diluted each mouse anti-human monoclonal antibody (used for the confirmation of purified recombinant protein) at room temperature for 1 h. After 30 min-incubation with 3000-fold-diluted goat anti-human IgG or anti-mouse IgG conjugated with alkaline phosphatase (AP), specific reactivity was estimated by the intensity with which each strip was stained with AP color development solution. The 22 kDa and 38 kDa immunostained bands were visualized for MuSK Ig1/2 and CRD monoclonal antibodies, respectively. When the serum sample showed the immunostained band at the same migration position as that proved with the test monoclonal antibody in the serum dilutions more than 1:500, the result was judged as antibody-positive.

3. Results

In the study collecting the serum samples from 43 anti-AChR-negative MG patients, 10 patients were negative for MuSK antibodies determined by both the standard RIA and the present study (group 3 in Table 1). All of the remaining 33 patients positive for MuSK antibodies determined by RIA were positive for MuSK Ig1/2 antibodies (groups 1 and 2 in Table 1); 10 patients of them (30%) were additionally positive for MuSK CRD antibodies (group 1 in Table 1). None was positive for MuSK CRD antibodies alone. Ten disease controls (anti-AChR-positive MG; group 4 in Table 1) and 10 healthy volunteers were all negative for MuSK Ig1/2 and MuSK CRD antibodies as well as for standard RIA-determined MuSK antibodies. The disease severity (MGFA grades) and clinical symptoms in each group showed that a trend was noted toward severe severity

Table 1
Clinical and immunological profiles of 53 myasthenia gravis (MG) patients.

Groups (numbers of patients)	1 (10)	2 (23)	3 (10)	4 (10)
Age at onset (years)	22–75	6–80	20–65	18–70
Gender	F 8/M 2	F 15/M 8	F 7/M 3	F 8/M 2
Antibodies against				
• MuSK Ig1/2 domains (immunoblot)	Positive	Positive	Negative	Negative
• MuSK CRD (immunoblot)	Positive	Negative	Negative	Negative
• Full-length of MuSK extracellular segment, determined by standard RIA (control, <0.05 nM)	6.08–131.40 nM	5.32–45.75 nM	<0.05 nM	<0.05 nM
• AChR, determined by standard RIA (control, <0.2 nM)	<0.2 nM	<0.2 nM	<0.2 nM	5.6–77.0 nM
MG severity (MGFA grades)				
IIa	0	3	4	0
IIb	0	7	2	3
IIIa	0	2	4	6
IIIb	4	1	0	1
IVa	0	0	0	0
IVb	0	0	0	0
V	6	10	0	0
Clinical symptoms				
Facial/bulbar weakness	10	20	2	4
Respiratory crisis	5	10	0	0
Neck weakness	5	2	0	0
Ophthalmoplegia	9	21	10	10
Limb weakness	6	13	10	7

F: female. M: male. MuSK: muscle-specific tyrosine kinase (Ig1/2 domains: immunoglobulin-like 1 and 2 domains; CRD: cysteine-rich domain). AChR: acetylcholine receptor. RIA: radioimmunoassay. MGFA: Myasthenia Gravis Foundation of America. Figures in MG severity and clinical symptoms indicate numbers of the patients subject to each item.

in anti-MuSK-positive MG (groups 1 and 2 in Table 1). However, there was no significant correlation between the positive (group 1 in Table 1)/negative (group 2 in Table 1) results from MuSK CRD antibody determination and the MGFA grades (Wilcoxon test, $p = 0.0747$). Representative immunoblots are shown in Fig. 1: C corresponding to group 1 and D corresponding to group 2 in Table 1. No immunostained band for MuSK Ig1/2 and MuSK CRD was seen with the serum from an anti-AChR-positive MG patient (B corresponding to group 4 in Table 1). The antibody specificity was confirmed by the same migration positions as those of purified, CBB-stained recombinant proteins (A in Fig. 1).

4. Discussion

This brief report shows that MuSK antibodies in a part of MG patients recognize not only the main immunogenic site(s) (Ig1/2 domains) responsible for the agrin signaling (McConville et al., 2004) but also the CRD responsible for the Wnt signaling (Stiegler et al., 2009). However, it remains to study as to whether the antibody heterogeneity could correlate with disease activity or characteristics.

Recent studies highlight Wnt involvement in critical aspects of the NMJ function and structure (Korkut and Budnik, 2009; Wu et al., 2010). Wnts 11 (Jing et al., 2009; Zhang et al., 2012), 9a (Zhang et al., 2012), 4 (Strochlic et al., 2012) and 3 (Henriquez et al., 2008), which are released from neurons or derived from muscles, bind to MuSK CRD and contribute to the AChR clustering via the Dvl-mediated noncanonical Wnt signaling cascade (Luo et al., 2002; Korkut and Budnik, 2009; Wu et al., 2010; Zhang et al., 2012). Therefore, the Wnt–Dvl signaling via MuSK CRD converges upon the agrin–Lrp4 signaling via MuSK Ig1/2 domains, and both contribute to AChR clustering. Therefore, our results suggest that MuSK CRD antibodies could be involved in impairment of the Wnt–MuSK interaction, suggesting a diversity to MuSK-implicated pathophysiology in MG.

Reportedly, the inhibited MuSK–Dvl interaction decreases the frequency of spontaneous synaptic currents (SSC) in association

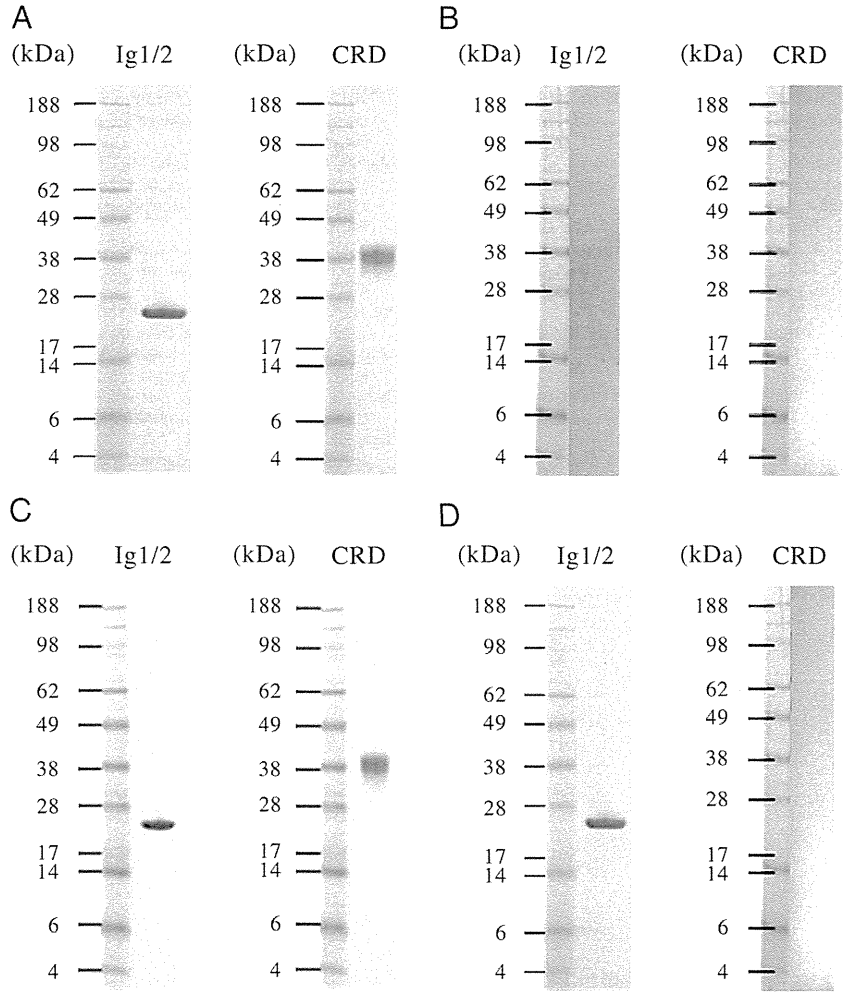

Fig. 1. Immunoblots of purified recombinant proteins of human MuSK extracellular segment (Ig1/2: immunoglobulin-like 1 and 2 domains; CRD: cysteine-rich domain) and immunostained reactivity with serum samples (1:500 dilution) from myasthenia gravis patients at 5 μg of recombinant protein/lane. A: Identification of purified, CBB-stained recombinant proteins (Ig1/2 domains: 1250 ng/lane; CRD: 2240 ng/lane). B: No reactivity was found for Ig1/2 domains and CRD with the serum from a 58 year-old man who was positive for AChR antibodies (9.8 nM), negative for MuSK antibodies (<0.05 nM) and MGFA-graded IIIb. C: Reactivity was found positive for both Ig1/2 domains and CRD with the serum from a 78 year-old woman who was negative for AChR antibodies (<0.2 nM), positive for MuSK antibodies (131.40 nM) and MGFA-graded V. D: Reactivity was found positive for Ig1/2 domains but negative for CRD with the serum from a 72 year-old man who was negative for AChR antibodies (<0.2 nM), positive for MuSK antibodies (45.75 nM) and MGFA-graded V. MuSK antibody titers shown in the parentheses were determined by the standard radioimmunoassay (RIA) (control,<0.05 nM). AChR antibody titers in the parentheses were also determined by conventional RIA (control, <0.2 nM).

with the decreased SSC amplitude in the NMJ, suggesting a defect in ACh release upregulation which may reflect retrograde Wnt signaling at the nerve terminal (Luo et al., 2002). The antibody-induced disturbance in bidirectional Wnt signaling via MuSK may, at least in part, be compatible with presynaptic abnormalities including the absence of ACh release upregulation to compensate for postsynaptic failure found in anti-MuSK-positive MG patients (Niks et al., 2010) and animal models (Cole et al., 2008; Richman et al., 2011; Klooster et al., 2012; Mori et al., 2012; Viegas et al., 2012).

We demonstrated that MuSK antibodies have heterogeneity in their binding to functional domains of MuSK. However, the present results cannot be informative to the significant difference in disease activity in MG patients who are MuSK Ig1/2 antibody-positive versus MuSK Ig1/2 and CRD antibody-positive. To establish the significance of MuSK CRD antibody specificity, the future studies need to include larger numbers of well-characterized patients, cell-based antibody assay, and passive and active immunization models.

Acknowledgments

The authors declare no conflicts of interest.

References

Cole, R.N., Reddel, S.W., Gervásio, O.L., Phillips, W.D., 2008. Anti-MuSK patient antibodies disrupt the mouse neuromuscular junction. Ann. Neurol. 63, 782–789.
Guptill, J.T., Sanders, D.B., Evoli, A., 2011. Anti-MuSK antibody myasthenia gravis: clinical findings and response to treatment in two large cohorts. Muscle Nerve 44, 36–40.
Henriquez, P.P., Webb, A., Bence, M., Bildsoe, H., Sahores, M., Hughes, S.M., Salinas, P.C., 2008. Wnt signaling promotes AChR aggregation at the neuromuscular synapse in collaboration with agrin. Proc. Natl. Acad. Sci. U. S. A. 105, 18812–18817.
Jaretzki III, A., Barohn, R.J., Ernstoff, R.M., Kaminski, H.L., Keesey, J.C., Penn, A.S., Sanders, D.B., 2000. Myasthenia gravis: recommendations for clinical research standards. Task Force of the Medical Scientific Advisory Board of the Myasthenia Gravis Foundation of America. Neurology 55, 16–23.
Jing, L., Lefebvre, J.L., Gordon, L.R., Granato, M., 2009. Wnt signals organize synaptic prepattern and axon guidance through the zebrafish unplugged/MuSK receptor. Neuron 61, 721–733.
Kim, N., Stiegler, A.L., Cameron, T.O., Hallock, P.T., Gomez, A.M., Huang, J.H., Hubbard, S.R., Dustin, M.L., Burden, S.J., 2008. Lrp4 is a receptor for agrin and forms a complex with MuSK. Cell 135, 334–342.
Klooster, R., Plomp, J.J., Huijbers, M.G., Niks, E.H., Straasheijm, K.R., Detmers, F.J., Hermans, P.W., Sleijpen, K., Verrips, A., Losen, M., Martinez-Martinez, P., De Baets, M.H., van der Maarel, S.M., Verschuuren, J.J., 2012. Muscle-specific kinase myasthenia gravis IgG4 autoantibodies cause severe neuromuscular junction dysfunction in mice. Brain 135, 1081–1101.
Korkut, C., Budnik, V., 2009. Wnts tune up the neuromuscular junction. Nat. Rev. 10, 627–634.
Luo, Z.G., Wang, Q., Zhou, J.Z., Wang, J., Luo, Z., Liu, M., He, X., Wynshaw-Boris, A., Xiong, W.C., Lu, B., Mei, L., 2002. Regulation of AChR clustering by Dishevelled interacting with MuSK and PAK1. Neuron 35, 489–505.

McConville, J., Farrugia, M.E., Beeson, D., Kishore, U., Metcalfe, R., Newsom-Davis, J., Vincent, A., 2004. Detection and characterization of MuSK antibodies in seronegative myasthenia gravis. Ann. Neurol. 55, 580–584.

Mori, S., Kubo, S., Akiyoshi, T., Yamada, S., Miyazaki, T., Hotta, H., Kishi, M., Konishi, T., Nishino, Y., Miyazawa, A., Maruyama, N., Shigemoto, K., 2012. Antibodies against muscle-specific kinase impair both presynaptic and postsynaptic functions in a murine model of myasthenia gravis. Am. J. Pathol. 180, 798–810.

Niks, E.H., Kuks, J.B., Wokke, J.H., Veldman, H., Bakker, E., Vershuuren, J.J., Plomp, J.J., 2010. Pre- and postsynaptic neuromuscular junction abnormalities in musk myasthenia. Muscle Nerve 42, 283–288.

Pasnoor, M., Wolfe, G.I., Nations, S., Trivedi, J., Barohn, R.J., Herbelin, L., McVey, A., Dimachkie, M., Kissel, J., Walsh, R., Amato, A., Mozaffar, T., Hungs, M., Chui, L., Goldstein, J., Novella, S., Burns, T., Phillips, L., Claussen, G., Young, A., Bertorini, T., Oh, S., 2010. Clinical findings in MuSK-antibody positive myasthenia gravis: a U.S. experience. Muscle Nerve 41, 370–374.

Richman, D.P., Nishi, K., Morell, S.W., Chang, J.M., Ferns, M.J., Wollmann, R.L., Maselli, R.A., Schnier, J., Agius, M.A., 2011. Acute severe animal model of anti-muscle-specific kinase myasthenia. Arch. Neurol. 69, 453–460.

Stiegler, A.L., Burden, S.J., Hubbard, S.R., 2006. Crystal structure of the agrin-responsive immunoglobulin-like domains 1 and 2 of the receptor tyrosine kinase MuSK. J. Mol. Biol. 364, 424–433.

Stiegler, A.L., Burden, S.J., Hubbard, S.R., 2009. Crystal structure of the Frizzled-like cysteine-rich domain of the receptor tyrosine kinase MuSK. J. Mol. Biol. 393, 1–9.

Strochlic, L., Falk, J., Goillot, E., Sigoillot, S., Bourgeois, F., Delers, P., Rouvière, J., Swain, A., Castellani, V., Schaeffer, L., Legay, C., 2012. Wnt4 participates in the formation of vertebrate neuromuscular junction. PLoS One 7, e29976.

Viegas, S., Jacobson, L., Waters, P., Cossins, J., Jacob, S., Leite, I., Webster, R., Vincent, A., 2012. Passive and active immunization models of MuSK-Ab positive myasthenia: electrophysiological evidence for pre and postsynaptic defects. Exp. Neurol. 234, 506–512.

Vincent, A., Leite, M.I., Farrugia, M.E., Jacob, S., Viegas, S., Shiraishi, H., Benveniste, O., Morgan, B.P., Hilton-Jones, D., Newsom-Davis, J., Beeson, D., Willcox, N., 2008. Myasthenia gravis seronegative for acetylcholine receptor antibodies. Ann. N. Y. Acad. Sci. 1132, 84–92.

Weatherbee, S.D., Anderson, K.V., Niswander, L.A., 2006. LDL-receptor-related protein 4 is crucial for formation of the neuromuscular junction. Development 133, 4993–5000.

Wu, H., Xiong, W.C., Mei, L., 2010. To build a synapse: signaling pathways in neuromuscular junction assembly. Development 137, 1017–1033.

Yamanashi, Y., Tezuka, T., Yokoyama, K., 2012. Activation of receptor protein-tyrosine kinases from the cytoplasmic compartment. J. Biochem. 151, 353–359.

Zhang, B., Luo, S., Wang, Q., Suzuki, T., Xiong, W.C., Mei, L., 2008. Lrp4 serves as a coreceptor of agrin. Neuron 60, 285–297.

Zhang, B., Liang, C., Bates, R., Yin, Y., Xiong, W.C., Mei, L., 2012. Wnt proteins regulate acetylcholine receptor clustering in muscle cells. Mol. Brain 5, 7.

BMC Medicine

RESEARCH ARTICLE Open Access

Efficacy of prosultiamine treatment in patients with human T lymphotropic virus type I-associated myelopathy/tropical spastic paraparesis: results from an open-label clinical trial

Tatsufumi Nakamura[1*†], Tomohiro Matsuo[2†], Taku Fukuda[3], Shinji Yamato[1], Kentaro Yamaguchi[4], Ikuo Kinoshita[5], Toshio Matsuzaki[6], Yoshihiro Nishiura[7], Kunihiko Nagasato[7], Tomoko Narita-Masuda[3], Hideki Nakamura[3], Katsuya Satoh[1], Hitoshi Sasaki[4], Hideki Sakai[2] and Atsushi Kawakami[3]

Abstract

Background: Human T lymphotropic virus type I (HTLV-I)-associated myelopathy/tropical spastic paraparesis (HAM/TSP) is a chronic myelopathy characterized by motor dysfunction of the lower extremities and urinary disturbance. Immunomodulatory treatments are the main strategy for HAM/TSP, but several issues are associated with long-term treatment. We conducted a clinical trial with prosultiamine (which has apoptotic activity against HTLV-I-infected cells) as a novel therapy in HAM/TSP patients.

Methods: We enrolled 24 HAM/TSP patients in this open-label clinical trial. Prosultiamine (300 mg, orally) was administered once daily for 12 weeks. We monitored changes in the motor function of the lower extremities and urinary function as well as copy numbers of the HTLV-I provirus in peripheral blood mononuclear cells (PBMCs).

Results: Improvement in the motor function of the lower extremities based on a reduction in spasticity (for example, decrease in time required for walking and descending a flight of stairs) was observed. In an urodynamic study (UDS), bladder capacity and detrusor pressure and then maximum flow rate increased significantly. Detrusor overactivity and detrusor-sphincter dyssynergia improved in 68.8% and 45.5% of patients observed at pretreatment, respectively. Improvement in UDS corresponded with improvements in the score of nocturia-quality of life questionnaire. HTLV-I proviral copy numbers in PBMCs decreased significantly (approximately 15.4%) compared with pretreatment levels.

Conclusions: These data suggest that prosultiamine can safely improve motor dysfunction of the lower extremities and urinary disturbance as well as reduce HTLV-I provirus levels in peripheral blood. It therefore has potential as a new therapeutic tool for HAM/TSP patients.

Trial registration: University Hospital Medical Information Network Clinical Trials Registry (UMIN-CTR) number, UMIN000005969.

Please see related commentary: http://www.biomedcentral.com/1741-7015/11/183.

Keywords: HAM/TSP, HTLV-I, Prosultiamine, Treatment

* Correspondence: tatsu@nagasaki-u.ac.jp
†Equal contributors
[1]Department of Molecular Microbiology and Immunology, Graduate School of Biomedical Sciences, Nagasaki University, 1-12-4 Sakamoto, Nagasaki 852-8523, Japan
Full list of author information is available at the end of the article

Background

Human T lymphotropic virus type I (HTLV-I) infects approximately 10 to 20 million people worldwide, mainly in large endemic areas such as southern Japan, the Caribbean, Central and South America, the Middle East, Melanesia, and equatorial regions of Africa [1,2]. HTLV-I is a human retrovirus and the causative agent of adult Tcell leukemia and HTLV-I-associated myelopathy/tropical spastic paraparesis (HAM/TSP) [3,4]. HAM/TSP is a chronic progressive myelopathy characterized by bilateral pyramidal tracts involved with sphincteric disturbances [5]. Only a small proportion of HTLV-I-infected individuals develop HAM/TSP. However, the main neurological symptoms (for example, motor dysfunction of the lower extremities accompanied by urinary disturbance) are progressive and lead to a deterioration in the quality of life (QoL) of patients once the myelopathy develops. Therefore, novel and safe therapeutic regimens are needed for HAM/TSP patients to use as treatment, or to prevent disease progression.

The primary neuropathological feature of HAM/TSP is chronic inflammation in the spinal cord caused by high HTLV-I proviral load in peripheral blood. Immunomodulatory therapy such as corticosteroid hormones and interferon (IFN)α has been the main treatment administered to HAM/TSP patients to date [6]. Although these treatments have produced good results in the short term, their overall efficacy is controversial [6,7]. In addition, it is not known if these treatments can be tolerated as a long-term or lifelong treatment against HAM/TSP, or whether they are necessary in the therapeutic strategy against HAM/TSP. When treating HAM/TSP, the optimal treatment is elimination of HTLV-I-infected cells from peripheral blood because HTLV-I-infected $CD4^+$ T cells are the first responders in the immunopathogenesis of HAM/TSP [8].

(*N*-[(4-amino-2-methyl-5-pyrimidinyl) methyl]-*N*-[4-hydoxy-1-methyl-2-(propyldithio)-1-butenyl]-formamide) is known as prosultiamine and as Alinamin®. It is a product of Takeda Pharmaceutical Company Limited (Osaka, Japan). Prosultiamine is a homolog of allithiamine, which was originally synthesized from thiol-type vitamin B1 and allicin [9]. For stability in the blood and efficient access of vitamin B1 to tissues, prosultiamine was developed after allyl disulfide derived from allicin was substituted with propyl disulfide in the structure of allithiamine [10]. Importantly, prosultiamine is pharmacologically stable and is readily available for the treatment of Wernicke's encephalopathy and polyneuropathy induced by deficiency of vitamin B1. Moreover, it has been shown to be safe for use in Japan. Therefore, this drug could be utilized immediately for conducting clinical trials in individuals with HAM/TSP.

Recently, we demonstrated that prosultiamine can induce the caspase-dependent apoptosis of HTLV-I-infected cells through disruption of intracellular redox reactions by a disulfide moiety in its structure [11]. Based on these data, we undertook a clinical trial based on the intravenous administration of prosultiamine in HAM/TSP patients with the purpose of targeting HTLV-I-infected cells [11]. We found that prosultiamine administration for 2 weeks was safe and induced clinical improvement. Examples of such improvement included a decrease in (i) spasticity of the lower extremities and (ii) levels of HTLV-I provirus in peripheral blood mononuclear cells (PBMCs) to 30% to 50% of pretreatment levels.

As mentioned above, we do not know if prosultiamine can be tolerated as a long-term treatment against HAM/TSP or indeed if it is necessary in the therapeutic strategy against HAM/TSP. Therefore, in the present study, we administered prosultiamine *via* the oral route for 12 weeks in subjects with HAM/TSP. We found that such treatment could result in (i) improved motor function in the lower extremities based on a decrease in spasticity, (ii) appreciable amelioration of associated urinary disturbance, and (iii) a decrease in the level of HTLV-I provirus in peripheral blood.

Methods

Ethical approval of the study protocol

This study protocol was approved by the clinical studies review boards of Nagasaki University Hospital (Nagasaki, Japan). The clinical trial was registered in the University Hospital Medical Information Network Clinical Trials Registry (UMIN-CTR) UMIN000005969. Written informed consent was obtained from all patients enrolled in the study for both participation in the study, and for inclusion of personal data as shown in Table 1.

Patients

We enrolled 24 HAM/TSP patients (17 women and 7 men; 31 to 80 years (mean ± SD; 60.1 ± 11.2 years)) who fulfilled criteria described previously [12]. The duration of illness was 3 to 51 years (mean ± SD; 20.9 ± 12.1 years). Motor function scores were rated from 0 to 13 according to the motor disability score described by Osame *et al.* [13]. Concomitant therapies such as immunomodulators and drugs for the neurogenic bladder were continued on the condition that the dose was kept constant during the study period. Intermittent self-catheterization with regard to voiding was noted except in cases 7, 8, 10, 17, 21, 22, and 24. Patient profiles are shown in Tables 1 and 2.

Study design

Treatment protocol

Prosultiamine was imported from Ildon Pharmaceutical Co., Ltd (Seoul, South Korea). Capsulated prosultiamine (300 mg, orally) was administered once daily for 12 weeks.

Table 1 Profile of HAM/TSP patients enrolled and improvement of motor function in the lower extremities 12 weeks after treatment

Case no.	Age (years)	Sex	Duration of illness (years)	Concomitant therapy			Intermittent self-catheterization	OMDS[a]		Spasticity of the lower extremities	
				Immunomodulator	Drug for neurogenic bladder			Before treatment	After treatment	Before treatment	Improvement[b]
					Anticholinergic	α1 blocker					
1	80	Female	23	No	Yes		Yes	6	6	Yes	Yes
2	64	Female	16	No	Yes		Yes	6	6	Yes	Yes
3	57	Male	51	PSL/ IFN-α	Yes		Yes	6	6	Yes	Yes
4	51	Female	36	No	Yes		Yes	9	9	Yes	Yes
5	67	Female	3	No			Yes	3	3	No	
6	61	Female	30	No			Yes	5	5	Yes	Yes
7	68	Female	12	No		Yes	No	4	4	Yes	Yes
8	64	Male	11	PSL		Yes	No	5	5	Yes	No
9	66	Male	23	PSL	Yes		Yes	9	9	Yes	Yes
10	76	Male	23	No			No	6	6	Yes	Yes
11	53	Female	7	No			Yes	6	6	Yes	No
12	62	Female	12	PSL		Yes	Yes	4	4	No	
13	44	Female	22	No			Yes	6	6	Yes	No
14	56	Male	10	No	Yes		Yes	5	5	Yes	Yes
15	71	Female	45	No	Yes		Yes	9	9	No	
16	78	Female	18	No	Yes		Yes	5	5	Yes	Yes
17	50	Female	19	No			No	5	5	Yes	Yes
18	63	Female	29	No	Yes		Yes	8	8	Yes	Yes
19	62	Female	9	PSL	Yes		Yes	8	8	Yes	No
20	60	Female	34	No	Yes		Yes	2	1	No	
21	46	Female	26	PSL		Yes	No	2	1	Yes	Yes
22	31	Female	7	No		Yes	No	4	3	Yes	Yes
23	56	Male	18	No			Yes	10	10	No	
24	56	Male	16	IFN-α			No	2	2	Yes	Yes
Remarks	mean ± SD; 60.1 ± 11.2		mean ± SD; 20.9 ± 12.1								% improvement: 78.9 (P = 0.0003)[c]

[a]Osame's motor function score (OMDS) was rated from 0 to 13 according to the disability grade [13].
[b]Improvement in spasticity of more than 1 grade according to the modifiedAshworth scale [14].
[c]Statistical significance was determined by the McNemar test.
IFNα interferon α, *PSL* prednisolone.

Table 2 Improvement of motor function in the lower extremities and urinary function 12 weeks after treatment

Case no.	Time required to walk 10 m (sec)			Time required to walk downstairs (sec)			Detrusor overactivity		Detrusor-sphincter dyssnergia	
	Before treatment	After treatment	% improvement	Before treatment	After treatment	% Improvement	Before treatment	After treatment	Before treatment	After treatment
1	26.5	21.6	18.5		N.E.		No	No	No	No
2	15.5	9.8	36.8		N.E.		Yes	No	No	No
3	11.5	10.5	8.7	8.6	7.7	10.5	Yes	No	Yes	Yes
4		N.E.			N.E.		Yes	No	Yes	Yes
5	5.3	4.9	7.5	3.8	3.7	2.6	No	No	Yes	No
6	5.9	6.2	−5.1	4.1	4.2	−2.4	No	No	Yes	No
7	8.9	9.5	−6.7	9.2	7.9	14.1	No	No	No	No
8	12.6	13.3	−5.6	9.5	8.6	9.5	Yes	No	Yes	Yes
9		N.E.			N.E.		Yes	No	No	No
10	20	25.1	−25.5		N.E.		No	No	No	No
11	29.5	32.5	−10.2		N.E.		Yes	No	Yes	Yes
12	6.6	6.9	−4.5	4.4	4.3	2.3	Yes	No	Yes	No
13	22.8	21.3	6.6		N.E.		Yes	No	No	No
14	15.4	11.3	26.6	14.3	11.4	20.3	No	No	No	No
15	N.E.	N.E.			N.E.		Yes	No	No	No
16	13.7	20.9	−52.6		N.E.		Yes	Yes	Yes	Yes
17	13.3	11.5	13.5	10.0	7.3	27	Yes	Yes	No	No
18		N.E.			N.E.		Yes	Yes	No	No
19		N.E.			N.E.		Yes	Yes	Yes	No
20	6.9	5.7	17.4	4.5	3.5	22.2	No	No	No	No
21	5.7	4.1	28.1	3.6	3.5	2.8	Yes	No	No	No
22	10.3	6.8	34	9.4	4.4	53.2	Yes	Yes	Yes	Yes
23		N.E.			N.E.		No	No	Yes	No
24	4.5	4.3	4.4	3.2	3.4	−6.3	Yes	No	No	No
Remarks								% improvement: 68.8 (P = 0.0094)[a]		% improvement: 45.5 (P = 0.0736)[a]

[a]Statistical significance was determined by the McNemar test. N.E.; not evaluated because of high OMDS.

Assessment of effect

Neurological assessment

We monitored changes in neurological signs, motor disability scores, time required for walking 10 m, and time required for walking down a flight of stairs at 4-week intervals. Spasticity of the lower extremities was graded using the modified Ashworth scale (MAS) [14].

Urological assessment

Subjective symptoms were evaluated using the scores of the Nocturia Quality of Life (N-QoL) questionnaire [15-17] at 4-week intervals. The N-QoL questionnaire comprised 13 items and dealt with daytime energy, worry, productivity, sleep, and vitality. The total score ranged from 0 (poorest QoL) to 100 (best QoL). The Duet® Logic G2 system (Mediwatch UK Ltd., Rugby, UK) was used for the urodynamic study (UDS). Bladder capacity, detrusor pressure, maximum flow rate, detrusor overactivity (DO) and detrusor-sphincter dyssynergia (DSD) were evaluated by UDS.

Quantification of HTLV-I proviral load

For quantitative analyses of HTLV-I proviral loads, real-time quantitative polymerase chain reaction (RT-qPCR) was carried out in a Light-Cycler® FastStart DNA Master (Roche Diagnostics, Mannheim, Germany) based on fluorescence detection with SYBER® Green, as described previously [11]. Briefly, genomic DNA samples from PBMCs from HAM/TSP patients were prepared using a Genomic DNA Extraction kit (Wako Pure Chemical Industries, Ltd., Osaka, Japan) and were subjected to RT-PCR in a LightCycler PCR system using *Tax*-specific primers, that is, forward primer (5′- AAACAGCCCTGCAGATACAAAGT-3′) and reverse primer (5′-ACTGTAGAGCTGAGCCGATAACG-3′), as well as β-actin-specific primers, that is, forward primer (5′-GCCCTCATTTCCCTCTCA-3′) and reverse primer (5′-GCTCAGGCAGGAAAGACAC-3′). The PCR condition for *Tax* was 40 cycles of denaturation (95°C, 15 s), annealing (55°C, 5 s), extension (72°C, 10 s). That for β-actin was 32 cycles of denaturation (95°C, 15 s), annealing (62°C, 5 s), and extension (72°C, 15 s). The HTLV-I proviral load per 10,000 cells was calculated according to the following formula: (copy number of *Tax*)/(copy number of β-actin/2) × 10,000

Statistical analyses

The Wilcoxon signed-rank test was used for statistical analyses of the change of HTLV-I proviral copy numbers and on the N-QoL scores or the urodynamic study except for DO and DSD. The McNemar test was used for statistical analyses of improvement of spasticity, DO and DSD. JMP 10 (SAS Institute Inc., Cary, NC, USA) was used as the software for statistical analyses. $P < 0.05$ was considered significant.

Results

Improvement of motor function of the lower extremities

Improvement in Osame's motor function score (OMDS) was observed in three patients during treatment (Table 1). After 12 weeks of treatment, improvement of more than 1 grade of the degree of spasticity (evaluated according to MAS) was observed in 15 of 19 patients in whom spasticity of the lower extremities was observed before treatment (% improvement; 78.9, $P = 0.0003$, McNemar test) (Table 1). In time required for walking 10 m in 18 ambulatory patients, the decrease ranged from 4.4% to 36.8% was observed in 11 patients although the increase ranged from 4.5% to 52.6% was observed in 7 patients (Table 2). In time required for walking down a flight of stairs in 12 patients, the decrease ranged from 2.3% to 53.2% was observed in 10 patients although the increase of 2.4% or 6.3% was observed in 2 patients (Table 2).

Improvement in urinary function

The conserved overall score of the N-QoL questionnaire was significantly improved, with a significant improvement of subscale scores at 12 weeks post treatment (Table 3). We compared urinary function by UDS at pretreatment with that at 12 weeks after treatment initiation. Bladder capacity and detrusor pressure were significantly increased from 341.3 (SD 127.2) ml to 391.0 (SD 139.9) ml ($P = 0.0097$), and 16.8 (SD 15.6) cm/H_2O to 27.5 (SD 15.3) cm/H_2O ($P = 0.0001$), respectively, by this treatment (Figure 1a,b). As analyzed in 18 patients whose own voiding function was partially reserved, the maximum flow rate was increased significantly from 7.5 (SD 6.2) ml/s to 10.2 (SD 5.6) ml/s ($P = 0.0139$) (Figure 1c). Moreover, DO improved in 68.8% (11 of 16 patients observed at pretreatment) by this treatment ($P = 0.0094$, McNemar test) (Table 2). DSD also improved in 45.5% (5 of 11 patients observed at pretreatment) 12 weeks after the start of treatment ($P = 0.0736$, McNemar test) (Table 2).

Decrease in HTLV-I proviral copy numbers in PBMCs

We monitored changes in copy numbers of the HTLV-I provirus in PBMCs at pretreatment as well as 4, 8, and 12 weeks after treatment commencement (Figure 2a). HTLV-I proviral copy numbers in 10^4 PBMCs decreased gradually from 2,127 (SD 1,932) at pretreatment to 1,961 (SD 1,692) ($P = 0.2776$, vs pretreatment), 1,845 (SD 1,693) ($P = 0.0152$, vs pretreatment) and 1,799 (SD 1,676) ($P = 0.0207$, vs pretreatment) at 4, 8, and 12 weeks after treatment, respectively. The level of HTLV-I proviral copy numbers 12 weeks after treatment decreased significantly (approximately 15.4%) from pretreatment levels. Figure 2b shows the changes in HTLV-I proviral copy numbers in each case between pretreatment and 12 weeks after treatment commencement. A decrease

Table 3 Changes in N-QoL scores after 12 weeks treatment with prosultiamine

Question	Before treatment	After treatment	*P*value
Q1 Concentration	0.6 ± 1.0	0.3 ± 1.6	0.1235
Q2 Low in energy	0.9 ± 1.1	0.4 ± 0.6	0.0077
Q3 Sleep during the day	1.5 ± 1.4	1.0 ± 1.1	0.0229
Q4 Productiveness	0.7 ± 0.9	0.3 ± 0.6	0.0830
Q5 Physical activities	1.0 ± 1.2	0.5 ± 0.8	0.0505
Q6 Fluid restriction	0.8 ± 1.2	0.7 ± 0.9	0.3270
Q7 Inadequate sleep at night	1.6 ± 1.5	0.7 ± 1.0	0.0070
Q8 Disturbance of others	0.8 ± 1.9	0.5 ± 1.8	0.0277
Q9 Preoccupation with waking at night	0.6 ± 1.1	0.3 ± 0.6	0.1235
Q10 Worry over condition worsening	1.5 ± 1.5	0.8 ± 1.1	0.0032
Q11 Worried over treatment options	1.5 ± 1.6	1.0 ± 1.3	0.0303
Q12 Overall bother	1.3 ± 1.3	0.8 ± 0.8	0.0238
Q13 Overall impact on everyday life	2.6 ± 2.8	0.9 ± 1.0	0.0023
Converted overall score (Q1 to 12)	73.2 ± 21.0	85.3 ± 19.9	0.0001
Subscale scores:			
Sleep/Energy (Q1 to5, 7)	74.0 ± 20.7	87.0 ± 15.0	0.0001
Bother/Concern (Q6, Q8 to12)	72.4 ± 25.7	83.7 ± 21.2	0.0028

Subjective symptoms were evaluated using the scores of the Nocturia Quality of Life (N-QoL) questionnaire [15-17]. The score ranges of each question except Q13 are from 0 to 4. The score of Q13 is from 0 to 10. Converted overall score (0–100) = 100 × total converted scores (Q1 to 12)/4 × question numbers, converted score = 4-each raw score. Subscale score (0 to 10) = 100 × total converted scores/4 × question numbers. Statistical significance was determined by the Wilcoxon signed-rank test.

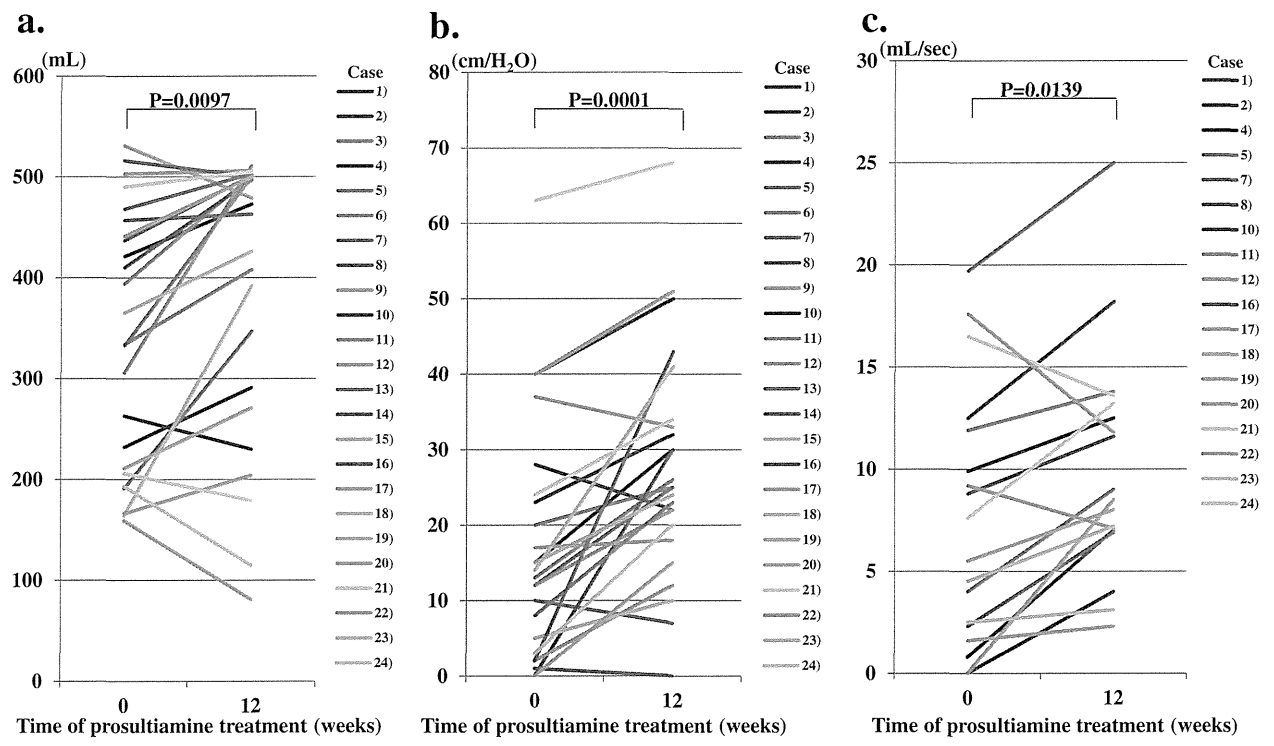

Figure 1 Change in bladder function as evaluated by urodynamic study. Bladder capacity **(a)** and detrusor pressure **(b)** increased significantly 12 weeks after prosultiamine treatment. Maximum flow rate **(c)** increased significantly 12 weeks after prosultiamine treatment as assessed in 18 patients whose voiding function alone was partially reserved. Statistical significance was determined by the Wilcoxon signed-rank test.